

Analysis of the fire resistance of timber jack arch flooring systems used in historical buildings

E. Garcia-Castillo, I. Paya-Zaforteza^{*}, A. Hospitaler

ICITECH, Universitat Politècnica de València, Camino de Vera s/n, 46022 Valencia, Spain

ARTICLE INFO

Keywords:

Timber jack arch flooring system
Fire resistance
Historical building
Heritage conservation
Resilience
Sustainability
2030 Agenda

ABSTRACT

Conservation of built heritage, at present, is a major task and a great challenge because it requires adapting the performance of existing buildings to current code requirements, when very often these were built before codes existed. Timber jack arch flooring systems can be found in many historical buildings around the world. The system is formed by timber joists and brick vaults spanning the distance between two adjacent joists and has an undoubtable aesthetic and cultural value. However, given its geometry, there is no methodology to verify its fire resistance, which has prevented the preservation of many buildings using this system. Within this context, this paper proposes a methodology based on the “Reduced cross-section method” included in Eurocode 5 (EN 1995-1-2) for the determination of the fire resistance of historical timber jack arch flooring systems subjected to different fire exposures. The methodology is based on the use of the 135-degree and the 300-degree isotherms to obtain the positions of the zero-strength layer and the charring depths, and is supported by both advanced numerical thermal models experimentally validated for standard fire exposure and advanced mechanical models. The methodology has been applied to a wide number of flooring systems covering different span lengths, timber static bending strengths, and fire exposures to evaluate the influence of these parameters on fire resistance. Results show that historical buildings do not always meet the requirements set by current codes and, therefore, performing these analyses is essential to ensure the fire resistance of these timber structures. By doing so, this work also contributes to cultural heritage conservation and to more sustainable construction in alignment with the fulfilment of United Nations 2030 Agenda’s eleventh goal: “Sustainable cities and communities”.

1. Introduction

According to the United Nations’ data, the current world population is 7700 million people and will reach 8500 million by 2030 and 9700 million by 2050 [1]. In addition, 55% of the current world population lives in cities, a percentage that will reach a value of 68% in 2050 [2]. Therefore, the world’s sustainability highly depends on the appropriate management of urban growth, especially considering that access to appropriate housing is one of the rights included in the Universal Declaration of Human Rights (UN, 1948) and thus, an important driving force in the political agenda of every country.

A combination of different options might provide the housing required both due to population growth and the lack of suitable housing, such as: 1) the construction of new houses in rural land transformed into urban land, 2) the construction of new houses in plots existing within the cities and 3) the rehabilitation of existing houses. When possible, and generally speaking, rehabilitation seems to be the best option when

social, environmental and cultural aspects are considered since: 1) rehabilitation is more labour intensive than the construction of new buildings and, therefore, the money invested goes mainly toward salary payments rather than the acquisition of materials and subsequent construction, 2) rehabilitation of existing buildings incurs a lower environmental impact than their replacement with the construction of new buildings (see e.g. [3]), 3) rehabilitation enables the conservation of traditional professions (specialized carpenters, stonemasons, blacksmiths...) which are generally not required by new building construction [4], 4) rehabilitation enables the conservation of built heritage and therefore of the traditional urban fabric and aesthetics of cities, 5) rehabilitation might even be more cost effective than new construction when the total life cycle of a building is considered [5]. Rehabilitation also presents challenges, one of the most important ones being adapting old buildings to present-day code requirements. One of these requirements is the need for a specified fire resistance. This requirement is especially challenging because most of the historical buildings were

^{*} Corresponding author.

E-mail addresses: esgarcas@upv.es (E. Garcia-Castillo), igpaza@upv.es (I. Paya-Zaforteza), ahospitaler@upv.es (A. Hospitaler).

<https://doi.org/10.1016/j.engstruct.2021.112679>

Received 2 November 2020; Received in revised form 9 April 2021; Accepted 3 June 2021

0141-0296/© 2021 The Authors. Published by Elsevier Ltd. This is an open access article under the CC BY-NC-ND license

(<http://creativecommons.org/licenses/by-nc-nd/4.0/>).

built at a time when fire codes did not exist.

Fire engineering has made significant progress in the development of performance-based approaches to deal with the effects of fire on buildings, tunnels and bridges built with different construction materials (see e.g. [6–14]). Regarding historic structures, recent fire research covers topics such as the propagation of fires within historical centres [15,16] or methodological approaches to fulfil fire safety requirements [17] and conduct post-fire restoration [18]. Specific research on the fire response of timber elements in historical buildings is very scarce and covers topics such as the estimation of the temperatures reached during a fire in timber structural elements [19] and the fire performance of certain heritage timbers compared to contemporary timbers [20,21]. On the contrary, the fire response of timber systems currently in use has got a lot of attention (see e.g. [22–28]), but timber structural systems used in historic buildings deserve special attention because: 1) they can have specific features that make the methods available in the codes not directly applicable, 2) timber used in historic buildings responds to fires differently than contemporary timber [20] and 3) many historic buildings with timber structural elements have suffered important damage and even collapsed due to fire as shown by the examples of the Notre Dame fire (2019) [29], the National Museum of Brazil fire (2018) [30], the Glasgow School of Art fires (2014, 2018) [31] and the 1988 Lisbon city Chiado's fire [32].

Within this context, this paper proposes a strategy for the determination of the fire resistance of a flooring system typical in historical buildings. By doing so, this work contributes to a more sustainable construction, to cultural heritage conservation, and to the fulfilment of one of the targets included in the 11th sustainable development goal on Sustainable Cities and Communities of the 2030 Agenda for Sustainable Development [33]: to strengthen efforts to protect and safeguard the world's cultural and natural heritage.

The type of flooring system studied is usually named as a timber jack arch flooring system and is defined by a series of brick arches supported by timber joists with different possible configurations ([34], Fig. 1a). The space between the arches or the joists and the floor top surface is filled with an infill of hydraulic mortar mixed with soil and brick rubble.

The timber joists are the main structural element of the floors and receive the loads from the brick arches or directly from the infill. This type of floors has an undoubtable aesthetic and cultural value (Fig. 1b), but, given its geometry, there is no simplified methodology in present codes to verify its fire resistance. This knowledge gap has resulted in the demolition or fireproofing (Fig. 1c) of many buildings with this system with the consequent environmental and social impacts and the loss of important heritage. This loss could have been avoided if proper fire resistance verification methods would have been developed and applied.

This paper proposes a simplified methodology to analyse the fire resistance of historical timber jack arch flooring systems. The methodology is based on calibrated numerical and simplified models and is applied to a wide number of flooring systems covering different span lengths, timber static bending resistance and fire loads. These fire loads have been obtained after a detailed study on the influence of the compartment size, ventilation conditions and fire models on the temperatures resulting from the fire. The results from this study on the fire loads are useful for any type of floor, not just for the typology analysed in the paper.

2. Case study

The timber jack arch flooring system analysed belongs to a four-storey residential building located in the historic centre of the city of Valencia (Spain). Fig. 2 shows the geometry of the flooring system, which is formed by rectangular timber joists, each joist having two timber strips nailed to it that support brick vaults. The wood of the joists comes from coniferous trees. Specifically, the wood belongs to the *Pinus nigra* species, which is a species of pine found in Mediterranean forests. In Mediterranean Europe, trees normally associated with this species include scots pine and laricio pine. The vaults between the joists are made of solid bricks joined with hydraulic lime mortar. Finally, the infill, which is located above the brick arches and is flush with the upper face of the joists, consists of a hydraulic lime mortar mixed with soil and brick rubble.

To make the analysis as representative as possible, three different

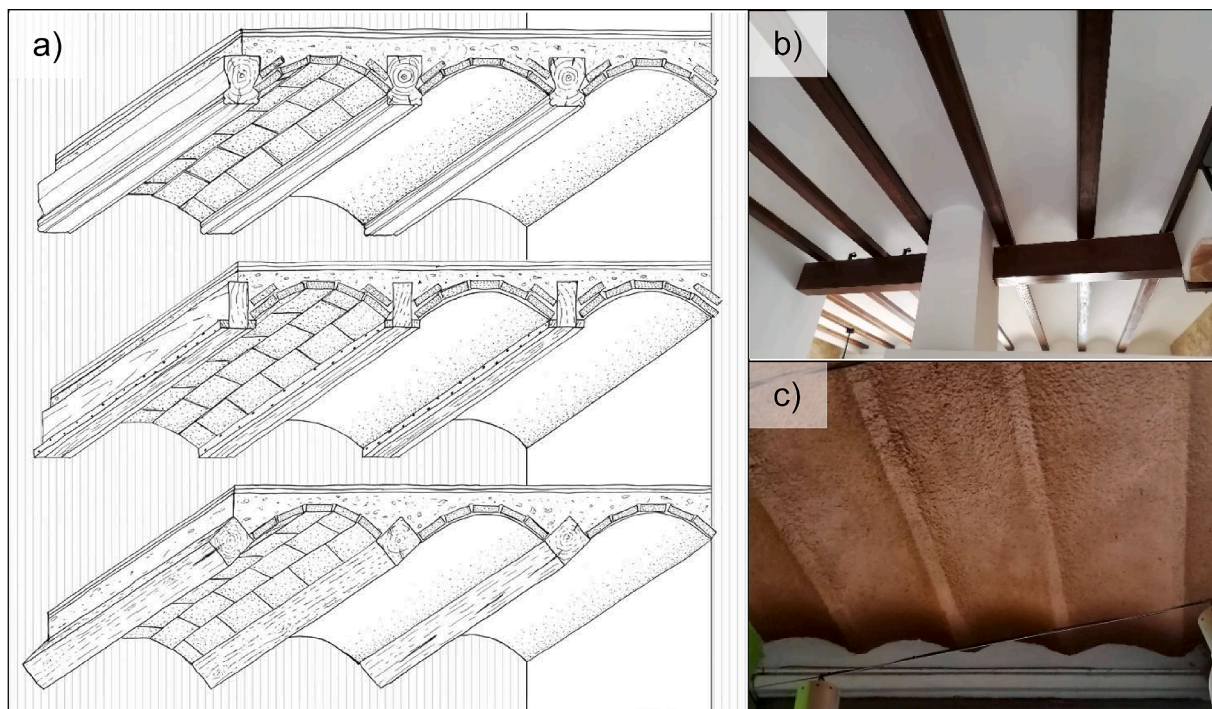


Fig. 1. Timber jack arch flooring systems: (a) joist variants – adapted from [35]; (b) general view of a jack arch flooring system with timber joists after rehabilitation; and (c) fireproofed jack arch flooring system.

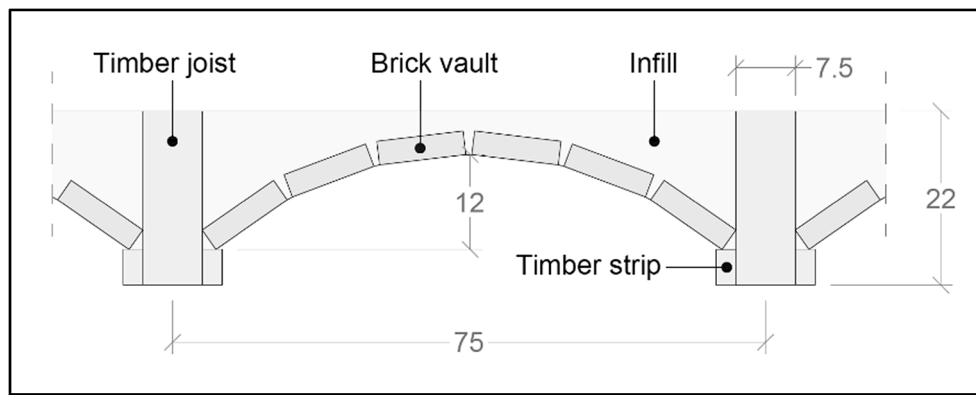


Fig. 2. Cross-section of the historical flooring system to be analysed. Dimensions in cm.

compartments of the building, in which the fire could occur and whose dimensions are typical of the different compartments that constitute a dwelling, have been considered in the analysis. The compartment 1 of 7 m² would be associated with a small bedroom, the compartment 2 of 16 m² with a double bedroom and, finally, the compartment 3 of 25 m² with a dining or living room. The span length of the flooring system is 4 m.

3. Basic safety requirements to be fulfilled

Since the residential building studied is located in Spain, the regulations included in the Spanish Building Code [36] (CTE henceforth according to its Spanish acronym) should be followed. This code establishes the requirements that buildings must meet in relation to basic safety and habitability requirements and applies to both new buildings and interventions in existing buildings. The CTE indicates that an element will have sufficient fire resistance if, during a certain time of exposure to the standard temperature–time curve, the design value of the effect of the actions, at any instant of time t , does not exceed the resistance value of that element. The fire resistance duration to be satisfied depends on the use of the building or compartment where the fire occurs as well as the most unfavourable evacuation height of the building. For residential buildings whose evacuation height is less than 15 m, a fire resistance duration of 60 min is required. For evacuation heights between 15 and 28 m, the duration to be satisfied is 90 min. Evacuation heights greater than 28 m are rarely reached in the constructive typology analysed. It should be noted that these values of fire resistance time are country dependent. Similar requirements are included in the codes of the countries having specific requirements for fire resistance (see e.g. [37]).

In this case, although the building under study has an evacuation height of less than 15 m, which requires a fire resistance duration of 60 min, the results obtained for a fire exposure time of 90 min will also be presented.

4. Methodology

The procedure established by EN 1991-1-2 [38] has been followed to analyse the fire resistance of the flooring system studied. First of all, the fire models to be considered in the thermal analysis must be selected. In this case, these are a selection of those proposed by EN 1991-1-2 [38]: the standard fire exposure (ISO 834 [39]); the parametric temperature–time curves (Annex A); and the two-zones models (Annex D). They are all described in depth in Section 4.1 of this article.

Next, the different compartments where the fire can occur within a dwelling building must be selected. As mentioned in Section 2, three different compartments of the building have been considered in the analysis whose sizes are of 7, 16 and 25 m², respectively. The characteristics of the compartment do not have any influence when the

standard ISO 834 fire exposure is considered but they have a great influence on both the parametric temperature–time curves and the two-zones models.

Then, a thermal analysis is performed to obtain the evolution of the temperatures inside the flooring system as a function of time. For this purpose, advanced heat transfer models have been developed using a finite element software. The numerical models have been calibrated from an experimental test. Both the experimental test and the thermal analysis conducted are described in detail in Section 4.2 of this article.

Lastly, in order to obtain the fire resistance time of the flooring system, three different mechanical methods have been used. Two of them consist of a sectional mechanical calculation based on an adaptation of the simplified mechanical methods of EN 1995-1-2 [40] used to verify the mechanical resistance of timber in a fire situation, whilst the third one corresponds to an advanced mechanical model developed in a finite element software. The latter is used to check the performance of the simplified strategies proposed which are based on the simplified mechanical methods of EN 1995-1-2 [40]. The mechanical analysis has been carried out considering an experimentally derived value of timber static bending strength. The methodology followed for the mechanical analysis of the historical flooring system studied is described at length in Section 4.3 of this article.

4.1. Fire models

As mentioned above, the fire models chosen, in order of increasing complexity, are the standard ISO 834 fire exposure, the parametric temperature–time curves and the two-zones models. These models define, as a function of time, the gas temperature in the environment of the fire exposed surfaces.

The standard ISO 834 fire exposure is defined in EN 1991-1-2 [38]. Temperatures in this curve only depend on the time of fire exposure and are given by Eq. (1). It is important to mention that the curve does not represent any real fire as it lacks a decay phase, however, it is commonly used as an international reference system to compare construction elements.

$$\Theta_g = 20 + 345 \log_{10}(8t + 1) \quad (1)$$

The equations for the parametric temperature–time curves are based on a thermal balance model of the compartment in which the fire is developed. Expressions for these curves are detailed in the Annex A of EN 1991-1-2 [38]. The curves include a heating phase until reaching the maximum temperature in the compartment, followed by a cooling phase whose decrease is linear.

The main parameters that govern the heating phase of the parametric curves are the fire load density related to the total surface area of the enclosure as well as its physical conditions. The fire load density depends on the type of occupancy of the compartment, since it determines the type of fuel that can be present within it and, consequently, the heat

of combustion of that fuel. The value of the characteristic fire load density per unit floor area ($q_{f,k}$) has been taken from Annex E of EN 1991-1-2 [38]. In this case, for a residential building, a value of 948 MJ/m² has been assumed. On the other hand, the factor δ_n , which in this case equals 0.78, has been obtained assuming that only normal firefighting measures are present and that there is a fire brigade off site (Table E.2 of EN 1991-1-2 [38]). Finally, according to Annex E of EN 1991-1-2 [38], a combustion efficiency factor equal to 0.8 has been assumed.

The physical conditions of the compartment considered in the formulation of the parametric curves are the compartment size; the ventilation conditions; and the thermal properties of the enclosure surfaces. The walls of the compartments are made of bricks and covered by a 15 mm thick layer of plaster, the floorings consist of ceramic tiles and the ceilings consist of the historical flooring system studied. According to Annex A of EN 1991-1-2 [38], the thermal properties of the compartment boundaries may be taken at room temperature. The thermal properties of the infill, the ceramic tiles and the plaster material have been taken from the catalogue of construction elements of the CTE [36]. Those for the wood and the bricks have been taken from EN 1995-1-2 [40] and EN 1996-1-2 [41], respectively, except for the wood density which has been obtained experimentally as described in Section 4.2.2. Table 1 summarises the thermal properties of the materials of the enclosure surfaces of the compartments at room temperature.

The opening factor (O), a parameter involved in both the parametric temperature–time curves and the zone models, represents the degree of ventilation of the fire compartment and EN 1991-1-2 [38] defines it as follows:

$$O = A_v \sqrt{h_{eq}} / A_t \quad (2)$$

where A_v is the area of the openings, h_{eq} is the height of the openings and A_t is the total area of enclosure surfaces. Table 2 summarises the geometry as well as the ventilation hypotheses considered for each compartment.

Two additional ventilation hypotheses, named *c* and *d*, were considered but later discarded as it was verified that they had no relevance in the analysis. First, hypothesis *c* was to assume both the window and the door closed, whilst hypothesis *d* was to assume the door open and the window closed. Obviously, hypothesis *c* was discarded since, at the beginning of the fire, the oxygen is rapidly consumed and, therefore, the fire does not fully develop. Besides, the parametric temperature–time curves are applicable as long as the value of the opening factor is within the range between 0.02 and 0.2 m^{1/2}. Therefore, given that the opening factor of hypothesis *c* equals zero, this ventilation scenario falls outside the scope of the parametric curves.

The reason for discarding hypothesis *d* is explained as follows. At a certain temperature within the compartment, the windowpane would burst, causing a change in ventilation conditions within the fire. According to the studies developed in [42], the failure criterion for total window breakage (not cracking, as this will happen earlier) of a windowpane is associated with an average gas temperature within the compartment of 320 °C. As a result, and according to numerical simulations with two-zone models, the fire curves obtained considering open windows from the beginning were very similar to those obtained considering the windows closed and shattering at a certain temperature. Hence hypothesis *d* was considered irrelevant due to its similarity to hypothesis *a*.

Table 1
Thermal properties of the materials of the enclosure surfaces.

	Timber	Bricks	Infill	Floor tiles	Plaster
Density (kg/m ³)	611.03	1800	1800	2000	800
Thermal conductivity (W/m/K)	0.12	0.42	1.3	1	0.3
Specific heat (J/kg/K)	1530	564	1000	800	1000

Table 2
Geometry and ventilation hypotheses considered for each compartment.

Compartment	Compartment height	Case	Door	Window	Opening factor
1 (7 m ²)	3.4 m	a	Open (2.15 m × 1 m)	Open (1.2 m × 1.2 m)	0.095 m ^{1/2}
		b	Closed	Open (1.2 m × 1.2 m)	0.032 m ^{1/2}
2 (16 m ²)	3.4 m	a	Open (2.15 m × 1 m)	Open (2 m × 1.2 m)	0.068 m ^{1/2}
		b	Closed	Open (2 m × 1.2 m)	0.030 m ^{1/2}
3 (25 m ²)	3.4 m	a	Open (2.15 m × 1 m)	Open (3.2 m × 1.2 m)	0.063 m ^{1/2}
		b	Closed	Open (3.2 m × 1.2 m)	0.040 m ^{1/2}

Fig. 3 shows the parametric curves obtained for each compartment and ventilation hypothesis (see Table 2). Under the same ventilation hypothesis, the larger the compartment size, the higher the temperatures reached within it, and the longer the duration of the heating phase. In addition, it is observed that for medium and large compartments, hypothesis *a* results in higher temperatures than hypothesis *b*, although the heating phase in hypothesis *b* has a longer duration.

Finally, the zone models are also included within the natural fire models of EN 1991-1-2 [38]. However, unlike the parametric curves, the zone models are considered to be advanced fire models since they take into account the properties of the gas, the mass exchange and the energy exchange in the compartment. Thus, numerical models of Computational Fluid Dynamics (CFD) simulations are required for the definition of these models. In this case, the software OZone [43,44] version 3.0.4, developed by the University of Liège, has been used to obtain the evolution of the gas temperatures in the compartment (from this point the zone models will be referred to as the OZone curves).

Just as for the parametric curves, the OZone curves also depend on the fire load density and the physical characteristics of the compartment. Therefore, the same parameters as those assumed for the parametric curves have been applied to the OZone curves.

Fig. 4 shows the OZone curves obtained for each compartment and ventilation hypothesis which coincide with those assumed for the parametric curves (see Table 2). Under the same ventilation hypothesis, the larger the compartment size, the higher the temperatures reached within it, and the longer the duration of the heating phase. Moreover, if the ventilation scenarios for the same compartment are compared, it can be observed that hypothesis *b*, which is associated with a lower degree of ventilation of the compartment than hypothesis *a*, involves a higher maximum temperature reached within the compartment and a longer duration of the heating phase. Note that the maximum compartment temperatures obtained with OZone match very well the maximum temperatures given by the parametric fire curves in hypothesis 1b, 2b and 3b. However, significant differences appear in hypothesis 1a, 2a and 3a. These differences could be attributed to: (1) the smaller accuracy of parametric curves when compared to the more advanced OZone models, (2) the fact that parametric fire curves do not always perfectly match fire test results and, according to Franssen [45], still can be improved, (3) the fact that the hypothesis 1a, 2a and 3a correspond to cases in the limit of application of the expressions of the parametric fire curves due to their limit opening factor (O_{lim}).

4.2. Thermal analysis

4.2.1. Experimental test

As mentioned in Section 4, an experimental test was performed at the testing facilities of the *Universitat Politècnica de València* (Spain) to

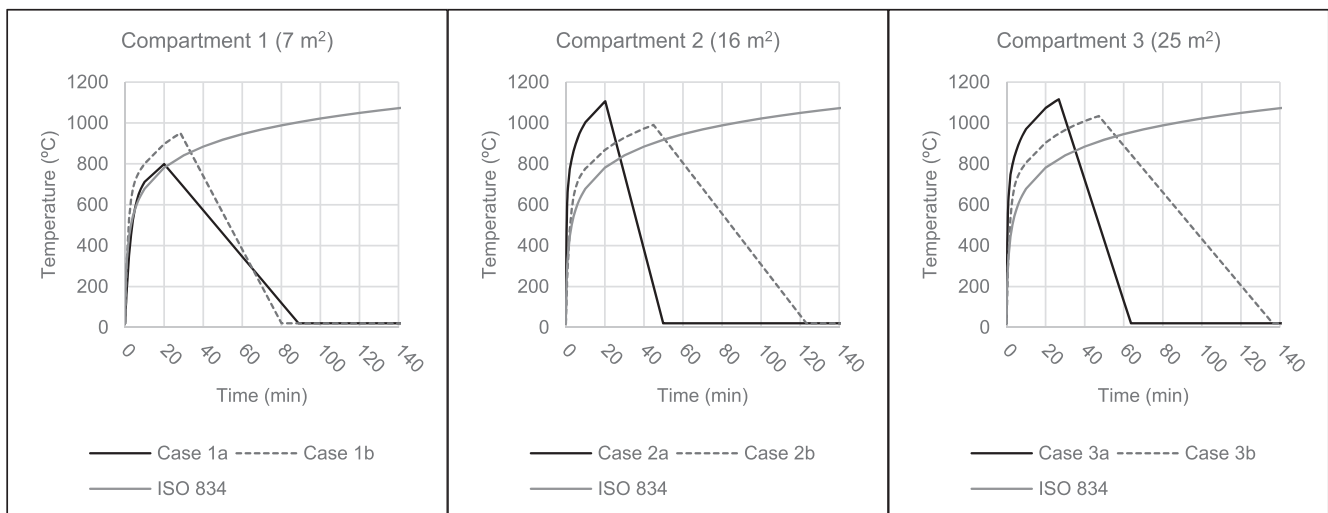


Fig. 3. Parametric temperature–time curves obtained for each compartment and ventilation hypothesis.

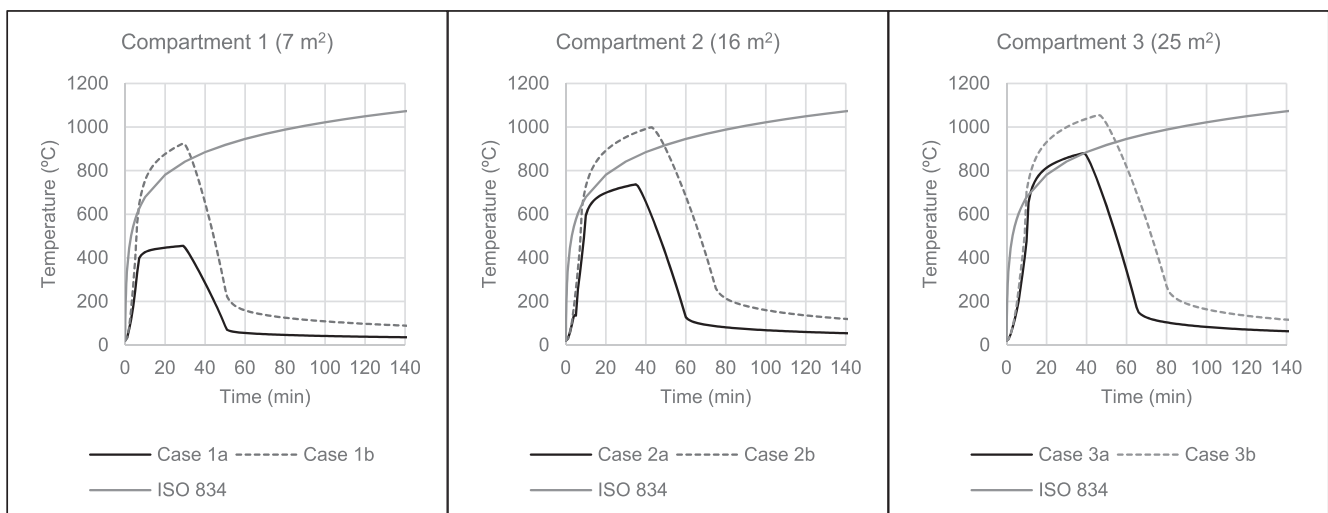


Fig. 4. Ozone temperature–time curves obtained for each compartment and ventilation hypothesis.

calibrate the finite element models developed for the thermal analysis of the flooring system. The thermal test was carried out using an electrical radiative furnace consisting of four electric radiative panels which are able to reach a maximum temperature in the order of 800 °C. Regarding their operation, a long-term target temperature is set on the electronic control of the panels and they are heated until reaching that target value. At this point, it is important to highlight that the panels are not able to follow a predefined time–temperature curve and that is why standard fire tests cannot be performed in this furnace. Further information on the characteristics of the furnace can be found in [46].

The geometry of the cross-section of the specimen which was tested is the one shown in Fig. 2. The length of the timber joists was 1.50 m, however, the length actually exposed was roughly one metre. The specimen was placed over the open side (top) of the furnace (see Fig. 5). This positioning reproduces a realistic fire exposure scenario since the heating of the flooring system only occurs from its lower surface. The gaps between the specimen and the side walls of the furnace were covered with thermal insulation to prevent as much heat loss as possible.

From the beginning of the test, the target temperature of each panel was set to the maximum value allowed (approximately 830 °C). For the purpose of recording the temperature evolution, four plate thermocouples were installed inside the furnace (see Fig. 5). These thermocouples

showed the homogeneity in the temperature distribution within the furnace. The temperature field evolution along the structure was also recorded using type K thermocouples throughout the thermal test. The specimen was built using three timber joists, however, only the central joist was instrumented with the aforementioned thermocouples. In particular, of the 38 type K thermocouples used, 22 were placed along the vertical plane of symmetry of the joist in order to register the temperature evolution at each centimetre of depth from the surface of the lower face of the joist up to 10 cm deep (see Fig. 6). The rest were placed in other areas such as the side strips as well as the contact surface between them and the joist; and, finally, in the infill. It is important to note that for each thermocouple position, there was also its symmetric one in order to have two measurements for the same relative point and, thus, verify that the temperatures recordings are correct.

Fig. 7 provides an overview of the experimental test performed. Temperatures over 800 °C were reached at the exposed timber joists. Therefore, the long-term temperature field reached in the structure throughout the test is in the same order of magnitude to that obtained from a real fire exposure.

The temperature–time curves obtained from the experimental test at different depths of the timber joist are presented in Fig. 8. The curves



Fig. 7. Experimental test: (a) furnace and timber elements instrumentation; (b) fire test; and (c) charring state of the timber joist after the test.

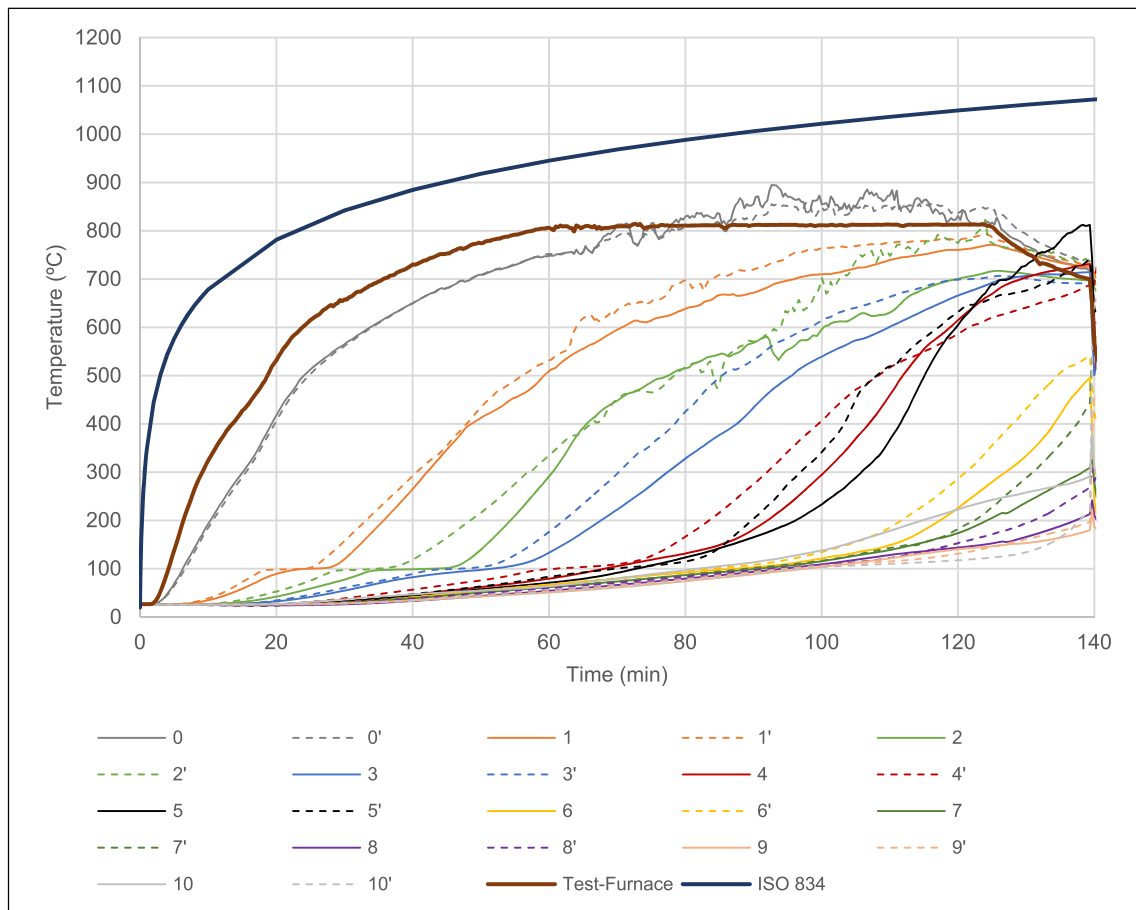


Fig. 8. Experimental test results. Temperature-time curves obtained for the thermocouple pairs from 0-0' to 10-10'. Thermocouples location is given in Fig. 6.

show a significant delay in the heating and, accordingly, in the charring of the wood, as can be deduced from the plateau observed in the experimental curves. This delay happens at around 100 °C and it is due to the fact that, at that temperature, most of the heat is used to evaporate the moisture in the wood and not to heat the joist. As justified in Section 4.2.2., this effect will be considered in the thermal model through the temperature-dependent specific heat curve of the wood. It is important to point out that this characteristic plateau has also been observed in other experimental fire tests carried out on timber elements (see e.g. [47,48]). As can be observed in Fig. 8, the furnace was turned off approximately 125 min after the experimental test began and the brick vaults of the specimen collapsed 15 min later.

4.2.2. Thermal modelling

The thermal analysis has been carried out with the software SAFIR [49,50] (v. 2019.a.2), developed at the University of Liège. This software is used to model the behaviour of building structures subjected to fire and applies the finite element method to perform both thermal and mechanical calculations.

In this case, a two-dimensional thermal analysis has been carried out. The analysis performed by SAFIR [49,50] is transitory, based on a non-linear calculation where the fire model is imposed on the exposed face of the flooring system and a room temperature of 20 °C is assigned on the unexposed one (see Fig. 9a).

The mesh of the model is shown in Fig. 9b and was generated by discretising each element of the flooring system into a certain number of finite elements. Since a 2D analysis has been performed, the finite elements are 2D-solid elements. Due to the irregular shape of the infill, triangular finite elements have been used to generate its mesh, whilst quadrilateral elements have been used to discretise the joist and the bricks. The use of concave elements has been avoided, since they do not provide reliable results. It is important to highlight that a sensitivity analysis of the assumed mesh has been carried out in such a way as to

have a reasonable computational cost, without compromising the accuracy of the results.

For the fire models considered, a uniform temperature distribution as a function of time can be assumed throughout the entire compartment, since they are not associated with localised fires. Consequently, all the structural elements of the same type will be uniformly affected by fire. Thus, it is sufficient merely to model and obtain the temperature field for a section of the flooring system including one joist and two half-vaults with their corresponding infill, delimited by the adiabatic edges in which there is no heat exchange.

The thermal properties of the flooring system materials introduced into the thermal model are the density (ρ), the thermal conductivity (λ) and the specific heat (c_p). Additionally, other parameters required by the thermal model are the wood moisture content, the emissivity (ε) and the coefficient of heat transfer by convection (α_c).

First, the density for the timber of the joists was obtained experimentally by testing 24 specimens according to EN 408 [51]. The average density was 611.03 kg/m³ (standard deviation: 28.22 kg/m³). Concerning the moisture content, a parameter on which both the density and the specific heat of the wood depend, it was also obtained experimentally by testing 24 specimens according to the methodology proposed by EN 13183-1 [52]. The average moisture content was 9.9% (standard deviation: 0.62%).

It has been assumed that both the density of the wood and the thermal conductivity are dependent on the temperature, in accordance with the curves proposed by Annex B of EN 1995-1-2 [40]. Regarding the temperature-specific heat curve proposed by EN 1995-1-2 [40], it shows a significant peak between 99 and 120 °C. This peak represents the heat consumed to evaporate the moisture in the wood and not to heat the material. Therefore, the energy consumed in the evaporation process depends on the moisture content of the wood. However, the temperature-specific heat relationship proposed by EN 1995-1-2 [40] for wood does not allow the actual value of moisture content of the

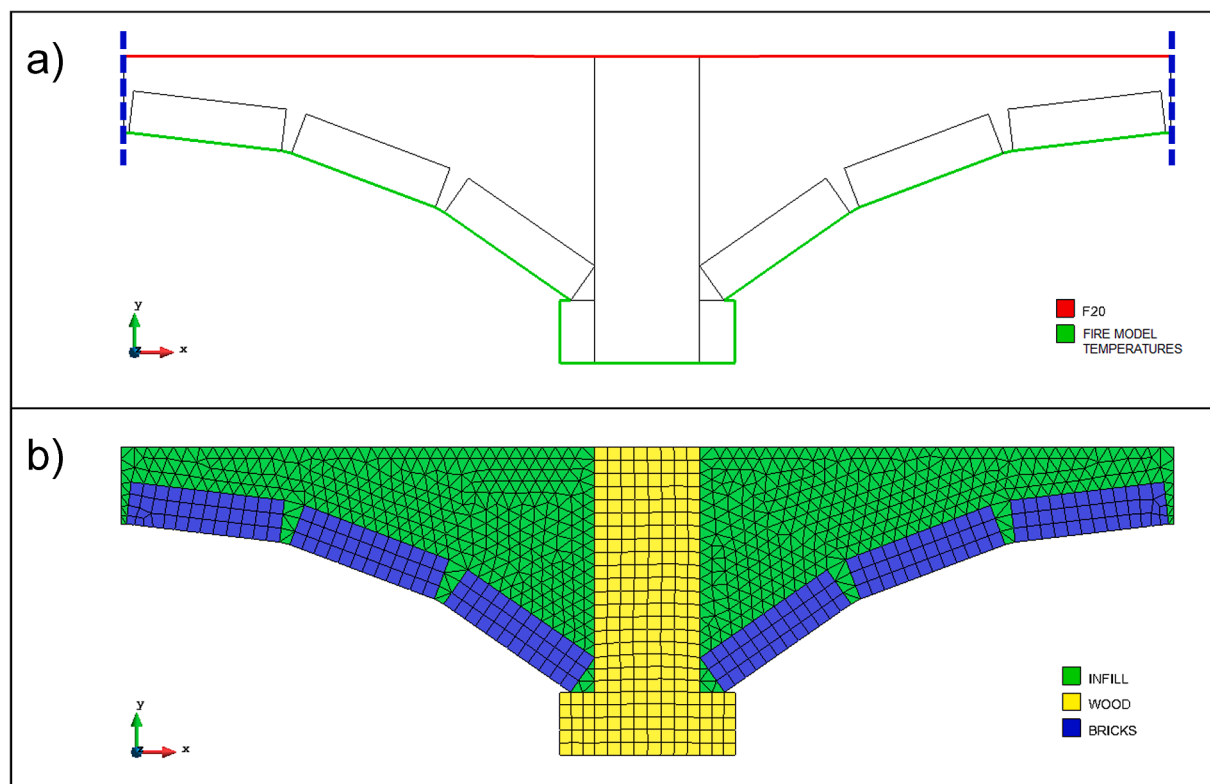


Fig. 9. FE thermal model: (a) boundary conditions (adiabatic edges in blue); and (b) materials and mesh generated. (For interpretation of the references to colour in this figure legend, the reader is referred to the web version of this article.)

material to be considered. That is why the methodology outlined in [53] by Wang et al. has been applied to modify the peak of the temperature-specific heat relationship of EN 1995-1-2 [40] for wood depending on the moisture content. As established by Annex B of EN 1995-1-2 [40] the modification of the wood thermal properties is allowed. Wang et al. [53] propose a triangular distribution of the peak and consider that the evaporation of water occurs between 90 and 150 °C (temperature range in which the peak develops). In this case, for a 9.9% moisture content, the equivalent triangular area of the peak, which represents the additional specific heat to evaporate the moisture in the wood, is 226 kJ/kg.

On the other hand, it is assumed that solid bricks have a density of 1800 kg/m³. Due to the nature of the material, unlike wood, this value of density will remain practically constant throughout the entire fire. However, both the thermal conductivity and the specific heat are dependent on the temperature, according to the curves proposed by Annex D of EN 1996-1-2 [41]. Fig. 10 summarises the thermal properties of both timber and bricks assumed in the thermal analysis.

The properties of the infill material have been taken from the catalogue of construction elements of the CTE [36]. According to this reference, the properties of the infill material (considering it as lime mortar) are: density equal to 1800 kg/m³, thermal conductivity equal to 1.30 W/m/K and specific heat equal to 1000 J/kg/K.

Lastly, according to EN 1995-1-2 [40], for wood surfaces, the emissivity coefficient is taken as 0.8. Regarding the coefficient of heat transfer by convection, EN 1991-1-2 [38] suggests considering a value of α_c equal to 25 W/m²K for the standard ISO 834 fire exposure and 35 W/m²K for simplified fire models (parametric curves) and for advanced fire models (two-zones models). For the calibration of the thermal model, a value of 35 W/m²K has been assumed and a sensitivity analysis has been carried out considering different values for this parameter.

It must be noted that the input fire curve used in this calibration model is equal to the average curve of the gas temperature recorded by the four plate thermocouples during the test, hereinafter referred to as furnace temperature–time curve.

To evaluate the differences between the temperatures as a function of time estimated by the numerical model at a given point and the temperatures obtained from the experimental test, the mean absolute error (MAE) and the root mean square error (RMSE) were used. Briefly, MAE provides an average of the differences in absolute value between the predictions and the test values, whereas RMSE represents the standard deviation of this difference. This methodology has been used before for similar applications within the field of fire engineering in civil engineering [54]. Eq. (3) and Eq. (4) define the MAE and RMSE, respectively.

$$MAE = \frac{1}{n} \sum_{i=1}^n |T_{esti} - T_{testi}| \quad (3)$$

$$RMSE = \sqrt{\frac{1}{n} \sum_{i=1}^n (T_{esti} - T_{testi})^2} \quad (4)$$

where T_{esti} is the estimated temperature at a particular point for an instant of time i ; T_{testi} is the test temperature at a particular point obtained from the experimental test for an instant of time i ; and n is the number of instants of time in which, during the experimental test, the temperature read by the thermocouples was recorded. Note that the errors have units of °C. In this case, given that the duration of the test was 140 min and the time interval set for temperature recording was 20 s, n takes a value equal to 421.

Since 11 pairs of symmetrical thermocouples were distributed along the vertical plane of symmetry of the joist to register the temperature evolution, the mean curve of the temperature recorded at symmetrical points was used to evaluate the errors of the numerical model at those eleven points. The MAE and the RMSE are obtained for each point and then, the errors obtained are averaged resulting in the values of MAE_{mean} and RMSE_{mean} for each calibration scenario.

Table 3 summarises all the numerical models studied, as well as the errors associated with each case. Case 1 was conducted to verify that the errors of the model assuming the Wang et al. [53] specific heat curve (case 2) were of the same order of magnitude as the errors of the model considering the EN 1995-1-2 [40] specific heat curve (case 1). As a result, the difference between the errors obtained in both cases is quite small, thus, the specific heat model of Wang et al. [53] chosen is validated. On the other hand, cases 3 to 6 correspond to the sensitivity analysis carried out for the coefficient of heat transfer by convection α_c . As can be deduced from Table 3, the numerical model is not very α_c -sensitive and as a result the value of α_c suggested by EN 1991-1-2 [38], 35 W/m²K, can be assumed. The reasons for this lack of sensitivity are explained next. The net heat flux on the fire exposed surfaces consists of two components, the net convective heat flux and the net radiative heat flux, which can be calculated according to EN 1991-1-2 [38]. These heat fluxes depend, among other factors, on the gas temperatures and the heated member surface temperatures. In the expression of the net

Table 3
Calibration scenarios and errors associated.

Case	c_p curve	$A_{cp,peak}$ (kJ/kg)	α_c (W/m ² K)	MAE _{mean} (°C)	RMSE _{mean} (°C)
1	EN 1995-1-2	243.7	35	34.25	46.32
2	Wang et al.	226	35	34.60	47.80
3	Wang et al.	226	25	34.01	46.62
4	Wang et al.	226	15	33.50	45.55
5	Wang et al.	226	5	33.40	44.72
6	Wang et al.	226	1	33.50	44.51

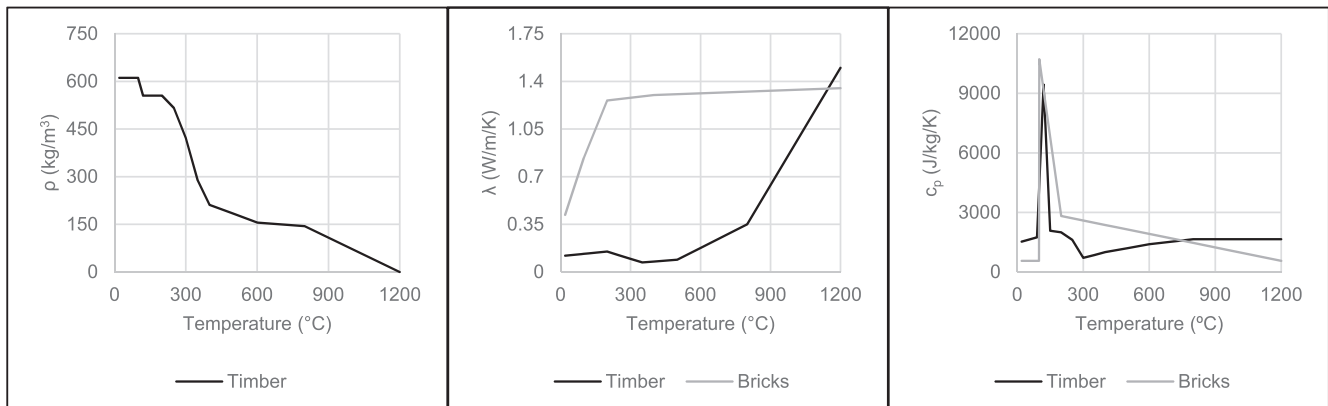


Fig. 10. Thermal properties of timber and bricks considered in the numerical model.

convective heat flux, where α_c appears, temperature terms are raised to the power of one. By contrast, in the expression of the net radiative heat flux, temperature terms are raised to the power of four. Therefore, as temperatures increase, radiation becomes dominant against convection. In the fire test analysed high temperatures are reached rapidly, and radiation prevails over convection after a short time of fire exposure. Consequently, the thermal model is not very sensitive to α_c .

It is worth noting that the peak's area of the specific heat curve of EN 1995-1-2 [40] is associated with a moisture content of approximately 11%. Since this value is very close to the one obtained experimentally (9.9%), it seems logical that the errors obtained for case 1 and case 2 are very similar.

Given that the experimental test performed is not a standard fire test, it has been verified that the furnace used is able to produce heating effects analogous to those produced by the standard ISO 834 fire exposure, since it is the fire model that current standards contemplate in fire resistance verification methods when a prescriptive approach is followed. For that purpose, from the existing time equivalent methods, a mechanical method based on the load capacity concept [55] has been used. In short, it consists of obtaining the time of exposure to the standard ISO 834 fire exposure for which the same fire resistance of the timber element subjected to a non-standard fire exposure is achieved. In this case, the analysis on the equivalent time of fire exposure has been carried out by means of the section modulus of the effective timber cross-section, i.e. the original cross-section reduced by both the charring depth and the thickness of the zero-strength layer (position of the 300-degree isotherm and thickness between the 300-degree and the 135-degree isotherms, respectively, as described in Section 4.3 and Section 5). In this way, it has been determined using the calibrated numerical model (case 2 in Table 3), that, approximately, 80 min of exposure to the furnace temperature–time curve produce the same heating effect (same section modulus of the effective timber cross-section) as 60 min of exposure to the standard ISO 834 fire exposure (see Fig. 11). Since the building studied must resist 60 min of the standard ISO 834 fire exposure, the validity of the experimental test carried out is confirmed. In fact, the experimental test heating lasted 125 min, therefore, the equivalent time of fire exposure actually reproduced is, approximately, 98 min.

Regarding the analysis on the equivalent time of fire exposure, it must be noted that both, thermal properties and heating rate of wood are dependent on the fire exposure [27]. In the case studied in this paper, the effective thermal properties obtained with the calibrated model have

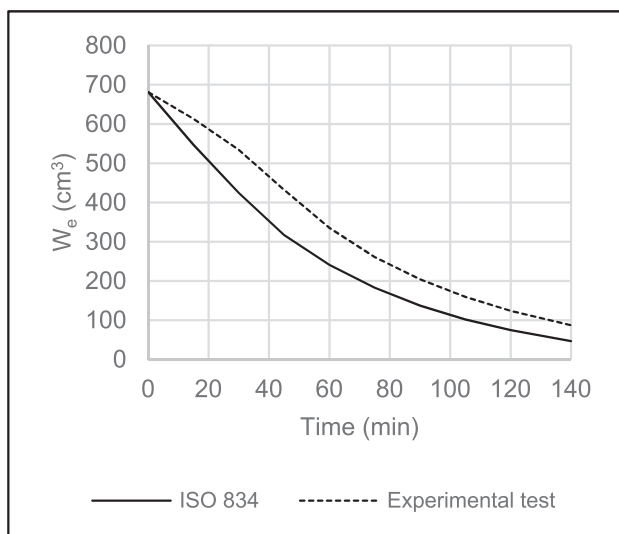


Fig. 11. Section modulus of the effective cross-section (W_e) of the timber joist throughout the time of fire exposure considering both the standard ISO 834 fire exposure and the experimental test fire exposure.

been experimentally derived for the experimental test fire exposure. However, these effective thermal properties are essentially those of EN 1995-1-2 [40] for wood, which are associated with the standard ISO 834 fire exposure, with minor changes in the temperature-specific heat relationship, which has been assumed according to Wang et al. [53] to better reproduce the plateau of temperatures that appears when timber reaches 100 °C. Therefore, the calibrated model is expected to reproduce the thermal behaviour of the wood under the standard ISO 834 fire exposure with accuracy, so comparison of the results obtained from both furnace and standard ISO 834 fire exposures is logical.

On the other hand, as mentioned previously, fire exposure has a great influence on the wood charring rate [27]. Therefore, the effective thermal properties considered in the calibrated thermal model, which have been experimentally derived for the furnace fire exposure, may not be able to accurately capture the thermal behaviour of wood under different fire exposures as well as during their decay phases. Consequently, the results obtained from the calibrated thermal model for natural fires (i.e. parametric fires and zone fire models) should be taken as indicative, as the calibration is based on the fire exposure of the experimental test. Since the thermal properties in EN 1995-1-2 [40] are very similar to those used by König and Walleij [56], a behaviour similar to the one reported by these authors should be expected. Therefore, temperatures from the calibrated numerical model should fit the temperatures produced in the timber section by fires with heating rates similar to those of the standard ISO 834 fire exposure (e.g. parametric curve 1a), might be conservative when the heating rate is higher (e.g. parametric curve 2a) and, finally, temperatures are probably underestimated during the decay phase.

Fig. 12 shows, for some of the positions of the thermocouple pairs, the comparison between the temperatures measured in the experimental test and the temperatures predicted by the numerical model. Note that the results of the numerical model have been represented with a tolerance of ± 3 mm (area shaded in orange) with respect to the theoretical position of the thermocouples. In short, as can be seen from the graphs of Fig. 12 and the MAE_{mean} and RMSE_{mean} values, the numerical model fits well with the curves obtained from the experimental test, including the reproduction of the plateau and the maximum temperatures reached at each point.

Fig. 13 shows the remaining cross-section of the central joist at mid-span after completion of the experimental test together with the original cross-section. Fig. 13 also shows the 300-degree, 200-degree and 135-degree isotherms obtained with the thermal numerical model of the experiment for a time of furnace fire exposure of 140 min, which coincides with the duration of the experimental test. The 300-degree isotherm is represented because it is a common adopted and accepted assumption in timber fire research that this temperature marks the position of the char-line [24,26,27,40], even though this position might vary with the wood properties (chemical composition, density, and moisture content) or fire exposure, among others [57]. The 200-degree isotherm is represented because the onset of pyrolysis is expected to happen at this temperature [26]. Finally, the 135-degree isotherm is represented because this temperature value marks the beginning of the zero-strength layer in the simplified mechanical method proposed in this paper as will be detailed in Section 5. Fig. 13 shows that the calibrated thermal model is able to reproduce the position of the charring front quite accurately, providing an additional validation of the numerical thermal model of the test.

4.3. Mechanical analysis

The mechanical analysis of the flooring system focuses on the timber joists since they are the main structural element and also the most vulnerable to fire. Therefore, the strength, and the stiffness of both the brick arches and the infill have been neglected. The loads considered in the mechanical analysis are the self-weight of the flooring system, the dead loads and the live load, the latter being given in the CTE [36],

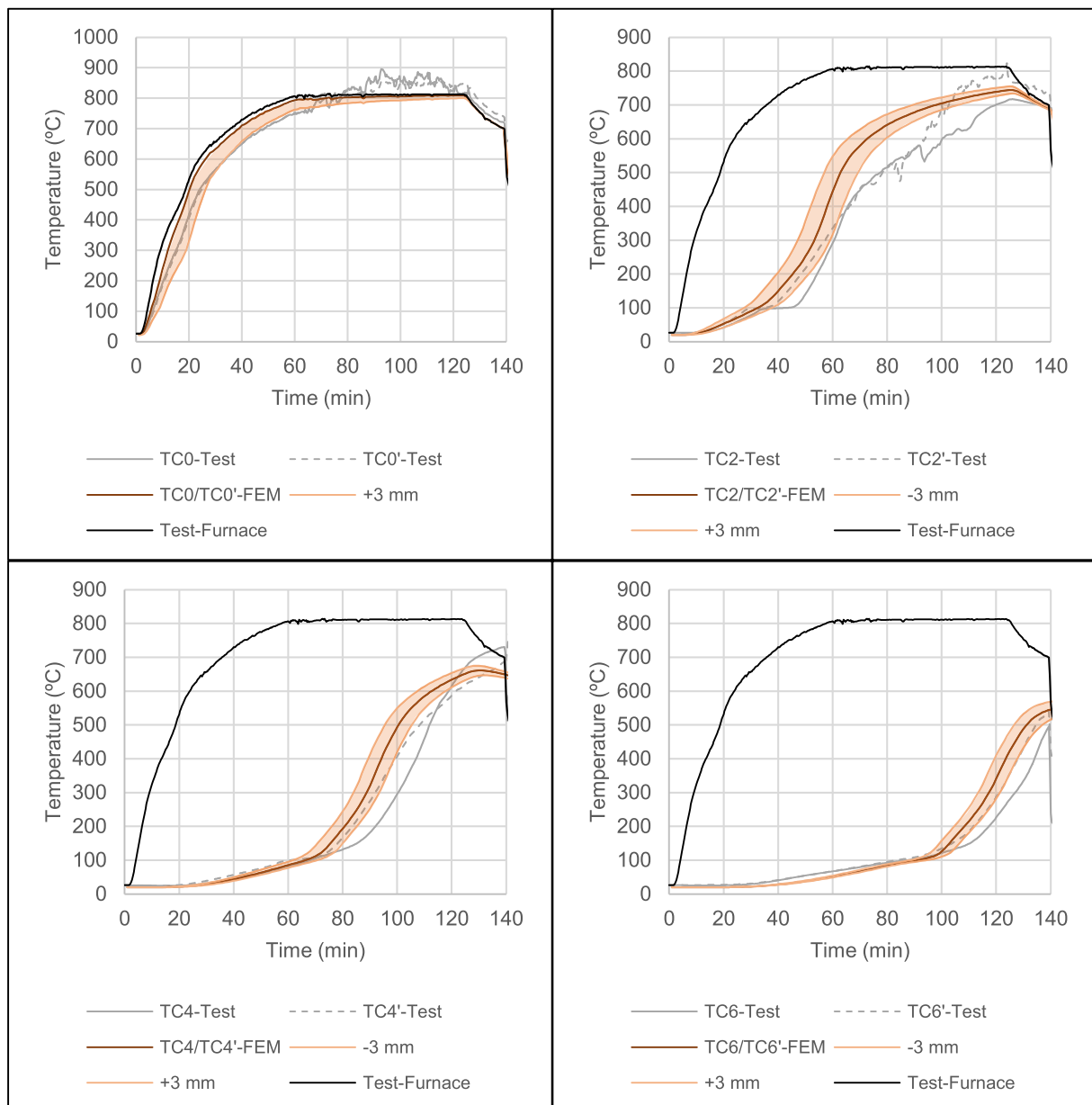


Fig. 12. Comparison between the experimental test and the numerical model (the results of the latter are represented with a tolerance of ± 3 mm).

which is in accordance with the value recommended by EN 1991-1-1 [58]. Table 4 summarises the values of the surface loads considered.

These loads are combined according to EN 1990 [59], using Eq. (5) (adapted from equation 6.11b of EN 1990 [59]) corresponding to accidental design situations in which only the action of a single variable load is expected:

$$\sum_{j \geq 1} G_{k,j} + (\psi_{1,1} \text{ or } \psi_{2,1}) Q_{k,1} \quad (5)$$

where $G_{k,j}$ is the characteristic value of permanent action j and $(\psi_{1,1} \text{ or } \psi_{2,1}) Q_{k,1}$ is the frequent or quasi-permanent value of the variable action, which, in this case, is the live load. Following the recommendation given in Section 4.3.1 of EN 1991-1-2 [38], the quasi-permanent value of the live load has been assumed. For live loads in residential buildings, EN 1990 [59] suggests considering a value of $\psi_{2,1}$ equal to 0.3. As a result of the combination of actions, and considering that the distance between the axis of two adjacent joists is 0.75 m, a linear load ($q_{d,fi}$) of 3.29 kN/m acting on each timber joist is obtained.

According to EN 1995-1-2 [40], the resistance of the structure to the combined action of fire and vertical loads can be obtained using advanced or simplified calculation models. Advanced calculation models make use of temperature dependent values of timber strength and modulus of elasticity and are described in Annex B of EN 1995-1-2 [40]. The simplified calculation methods for unprotected linear elements such as beams or columns considered in EN 1995-1-2 [40] are the “Reduced cross-section method” and the “Reduced properties method”. Both simplified methods have been developed for rectangular or T-shaped timber cross-sections submitted to the standard ISO 834 fire exposure and cannot be directly applied to jack arch flooring systems due to the singularity of their geometry and constituent materials. Therefore, advanced mechanical models implemented in SAFIR [49,50] have been used to propose and validate a simplified method based on the methods existing in EN 1995-1-2 [40].

The calculation of the fire resistance of the timber joist using advanced mechanical models carried out with SAFIR [49,50] is based on 2D beam finite elements whose cross-section includes the results of the

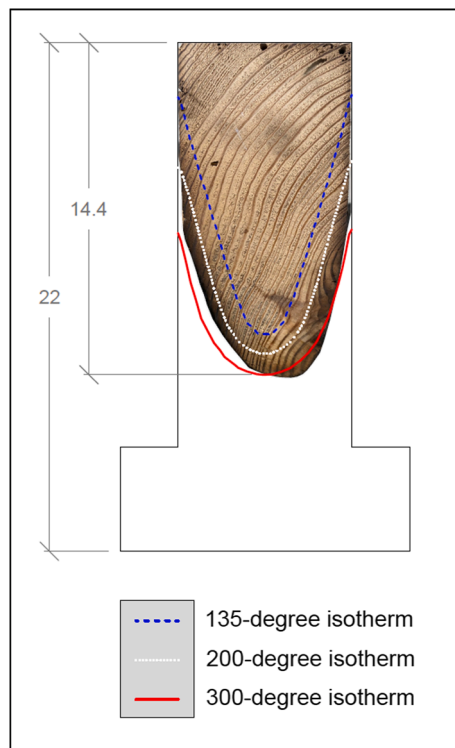


Fig. 13. Remaining cross-section of the central joist at mid-span after completion of the experimental test together with the original cross-section. Dimensions in cm.

Table 4

Loads considered in the mechanical analysis of the flooring system.

Load	Value (kN/m ²)
Self-weight	1.78
Tile floor	1.00
Partitions	1.00
Live load	2.00

thermal analysis that has also been developed in SAFIR [49,50]. The “pure Newton-Raphson” convergence procedure has been adopted for the calculations, as recommended in SAFIR’s manual [60] for structures made of beams. SAFIR [49,50] incorporates by default a uniaxial model for timber with the mechanical properties described in Annex B of EN 1995-1-2 [40]. This model considers the loss of strength and stiffness of the material as the temperature increases.

Taking into account the above considerations, the mechanical model consists of a simply supported beam with a pinned support at one end and a roller support at the other. After defining the geometry of the beam as well as its boundary conditions, both the load and the materials are assigned. Lastly, the 2D beam is discretised into 2D beam-type finite elements and the structural analysis is carried out. As a result, SAFIR [49,50] provides the evolution of deflections of the timber joist as well as its internal forces and stresses. Failure is assumed to happen when deflections become too large and, consequently, structural calculation stops because SAFIR [49,50] is unable to find a solution and converge. Note that for each fire model considered, a different mechanical model is required.

The simplified mechanical methods of EN 1995-1-2 [40] are based on the concept of charring depth. EN 1995-1-2 [40] defines it as the distance between the outer surface of the original timber member and the position of the char-line, the latter being the position of the 300-degree isotherm. EN 1995-1-2 [40] also proposes some equations for the

calculation of the charring depth for standard ISO 834 and parametric fire exposures. However, given the geometric singularity of the joists, as well as their boundary conditions, being partly surrounded by the infill of the flooring system, those equations cannot be applied directly in jack arch flooring systems and a numerical model to obtain the charring depths is necessary. Consequently, the 300-degree isotherm, as a function of the time exposure and obtained from the thermal model developed in SAFIR [49,50], has been used to obtain the charring depth. The cross-section of the original timber element reduced by the charring depth (d_{char}) is known as residual cross-section.

Once obtained the residual cross-section, the “Reduced cross-section method” proposes to consider an effective cross-section of the timber element in the mechanical analysis by removing from the residual cross-section parts of the cross-section with an assumed zero strength and stiffness. This removed thickness is also known as the zero-strength layer and intends to represent the effect of the reduction of strength and stiffness of the thermally affected timber behind the char front. The mechanical analysis can then be done using the effective cross-section with ambient temperature timber mechanical properties i.e. with a modification factor for fire ($k_{mod,fi}$) equal to 1.0. According to EN 1995-1-2 [40], for unprotected surfaces the thickness of the zero-strength layer is equal to a product of $k_{mod,fi}$ that, for fire exposure times exceeding 20 min, is equal to a maximum set value of 7 mm. However, the use of this fixed maximum value has been widely criticized. First, the value of 7 mm is associated with the standard ISO 834 fire exposure [61], therefore, it might be inaccurate for other fire exposures. In fact, it may be inaccurate and non-conservative even for some applications of the standard ISO 834 fire exposure and its revision covering a large scatter of wood properties as well as different loading modes and heating exposures is recommended in [62]. On the other hand, in the case of natural fires, thermal penetration depth keeps increasing during the cooling phase of a fire even when the charring front has halted, which affects the load bearing capacity of the timber element and could produce its collapse. Therefore, a fixed value of the thickness of the zero-strength layer cannot represent either the continuous thermal wave after the charring front has halted or the decay phase effects [24]. In an attempt to overcome these limitations, Richter et al. [26] have adopted the thickness between the 200-degree and the 300-degree isotherms as the thickness of the zero-strength layer. This limit was chosen because 200 °C coincides with the onset of pyrolysis [26], but the validity of the proposal was not verified using results of mechanical models. Following Richter et al. [26], a first attempt to adapt the “Reduced cross-section method” to the particularities of the case studied was done using the 200-degree isotherm to define the zero-strength layer and the effective cross-section. However, the results obtained did not match very well the advanced mechanical model results, because significant heat induced deterioration of timber mechanical properties occurs below 200 °C [24]. Therefore, and following one of the approaches suggested by Schmid et al. [62], the zero-strength layer has been obtained by comparing the load-bearing capacity of the heated cross-section with temperature-dependent material properties obtained with the advanced numerical model and thus non-linear stress distribution, with the load bearing capacity of an effective timber cross section obtained using a linear-elastic approach and ambient temperature material properties. Details of this analysis are given in Section 5 and show that the use of the 135-degree isotherm instead of the 200-degree isotherm to define the position of the zero-strength layer gives much better results.

On the other hand, the “Reduced properties method” proposes to consider the residual cross-section as the resistant section for the mechanical analysis. However, the design strength and stiffness properties should be reduced by a factor $k_{mod,fi}$. In this method, this factor depends linearly on the geometric properties of the residual cross-section, which, in turn, vary depending on the time of fire exposure. The expressions to obtain the values of $k_{mod,fi}$ are indicated in EN 1995-1-2 [40].

Therefore, when simplified mechanical methods are used, once the corresponding isotherms are obtained in SAFIR [49,50] for each fire

model considered, a sectional calculation is performed to obtain the maximum load ($q_{Rd,fi}$) that the flooring system can bear in accidental situations of fire exposure. The value depends on the span of the flooring system (4 m in this case) and is calculated considering that the flooring systems are simply supported. In brief, for each instant of time t ; fire model; and simplified mechanical method a different value of $q_{Rd,fi}$ is obtained (see Eq. (6)).

$$q_{Rd,fi} = \frac{8 M_{max}(t)}{L^2} = \frac{8 [f_{d,fi} \cdot (W_{ef}(t) \text{ or } W_r(t))]}{L^2} \quad (6)$$

where $M_{max}(t)$ is the maximum bending moment that the residual cross-section of the simply supported timber joist can bear at a given instant of time t of the fire exposure, L is the span length of the flooring system, $f_{d,fi}$ is the static bending design strength of timber in fire and $W_r(t)$ and $W_{ef}(t)$ are the section modulus of the residual cross-section for the reduced properties method and the section modulus of the effective cross-section for the reduced cross-section method, respectively, at a given instant of time t of the fire exposure. The mechanical properties required to obtain these section moduli for each time step t are obtained using CAD software. The degree of compliance of the flooring system with the standards can then be expressed through safety factors (SF), depending on the time of exposure to the different fire models considered. These safety factors are obtained as the relation between the maximum load ($q_{Rd,fi}$) that the timber joist can bear for the accidental situation of fire exposure and the linear load ($q_{d,fi}$) acting on each timber joist. Therefore, values of the safety factor equal or higher than one imply the fulfilment of the regulatory requirements regarding the fire resistance time of the element.

The fundamental parameters of the structural model are the timber strength to static bending and its Young's modulus. For the timber used in the joists of the case study, these parameters have been obtained with four four-point bending tests carried out on a universal testing machine

INSTRON 3382 following the methodology described in EN 408 [51] (see Fig. 14). From these tests, a mean value of bending strength of 69.79 MPa (standard deviation: 3.28 MPa) has been obtained and a Young's modulus of 12029.19 MPa. These values correspond to a high-quality timber according to bibliography [63].

It is important to highlight that, apart from the failure mode due to the cross-section having exceeded its maximum load bearing capacity, a possible additional failure mode, which consists of the loss of support of the brick vaults due to the charring of the timber joists, must be taken into account. In this work, it has been considered that the support of the brick vaults could be lost when the charring front (300-degree isotherm) reaches the line that passes through the last point of the brick vaults remaining in contact with the timber joist (see the horizontal red line in Fig. 15).

5. Results and discussion

This section shows and discusses results of both the thermal and mechanical analyses performed. It also provides a validation of the simplified strategy proposed.

The purpose of the thermal analysis carried out in SAFIR [49,50] is twofold. First, this analysis provides the evolution of the temperatures within the timber joist, which are required to perform the advanced mechanical calculations using temperature dependent mechanical properties. Secondly, the thermal analysis also enables to obtain the 135-degree and 300-degree isotherms on the timber joists' cross-section, which are required for the mechanical analysis using the simplified strategy proposed in this paper. By way of example, Fig. 16 presents the results for the standard ISO 834 fire exposure, specifically, it shows the temperature fields for times of fire exposure of 30, 60 and 90 min. Similarly, Fig. 17 shows the results of the mechanical analysis performed in SAFIR [49,50] after 60 min of standard ISO 834 fire exposure. It can be observed that the normal stresses to which the joist is subjected are well below the strength of the timber.

To validate the simplified strategy proposed, the fire resistance times and the evolution of the deflections for the case study analysed heated with different fire exposures have been obtained using advanced mechanical models and the strategy proposed. Results obtained using the "Reduced cross-section method" include two cases depending on whether the position of the zero-strength layer is obtained using the 200-degree isotherm as suggested in [26] or using the 135-degree isotherm as proposed in this work. The goal of comparing these results is to check the ability of the proposed adaptations of the simplified methods to predict the fire response of the structural system analysed in the theoretical case where failure due to the loss of support of the brick vaults does not happen. Table 5 shows the fire resistance predictions for the ISO 834, P-3b and O-3b fire exposures. These fire exposures have been selected because they constitute the cases in which structural failure occurs within the first 120 min of fire exposure. Results obtained using the strategy with the 135-degree isotherm match remarkably well advanced numerical model results whereas the 200-degree isotherm and the strategy based on the reduced properties method provide unconservative results. Fig. 18 shows the evolution of the timber joist mid-span deflections for the ISO 834, P-3b and O-3b fire exposures. The three simplified approaches can approximate the pattern of the evolution of the deflections but, again, the reduced-cross section method with the 135-degree isotherm provides the most accurate results. As a consequence, this method is proposed as simplified strategy to obtain the fire resistance of the flooring system.

Fig. 19 summarises the results of the mechanical analysis of the flooring system according to the proposed adaptation of the "Reduced cross-section method" with the 135-degree isotherm. Only the most unfavourable fire models have been considered in the mechanical analysis. These are the standard ISO 834 fire exposure and the parametric and OZone curves associated with compartment 3. The latter are characterised by a longer duration of the heating phase as well as higher



Fig. 14. Four-point bending test carried out.

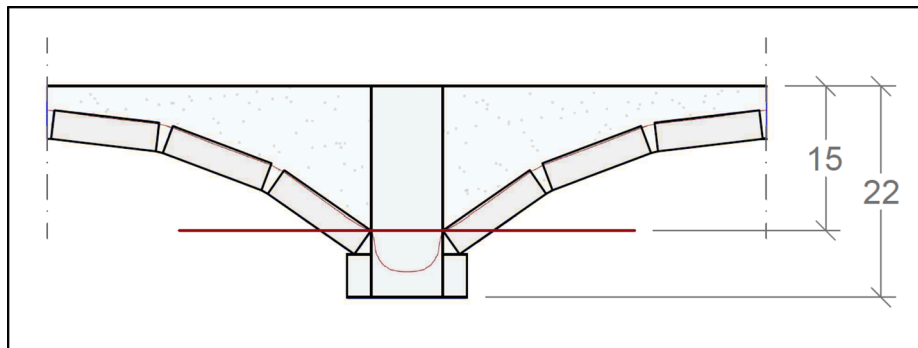


Fig. 15. Failure criterion for the failure mode corresponding to the loss of support of the brick vaults.

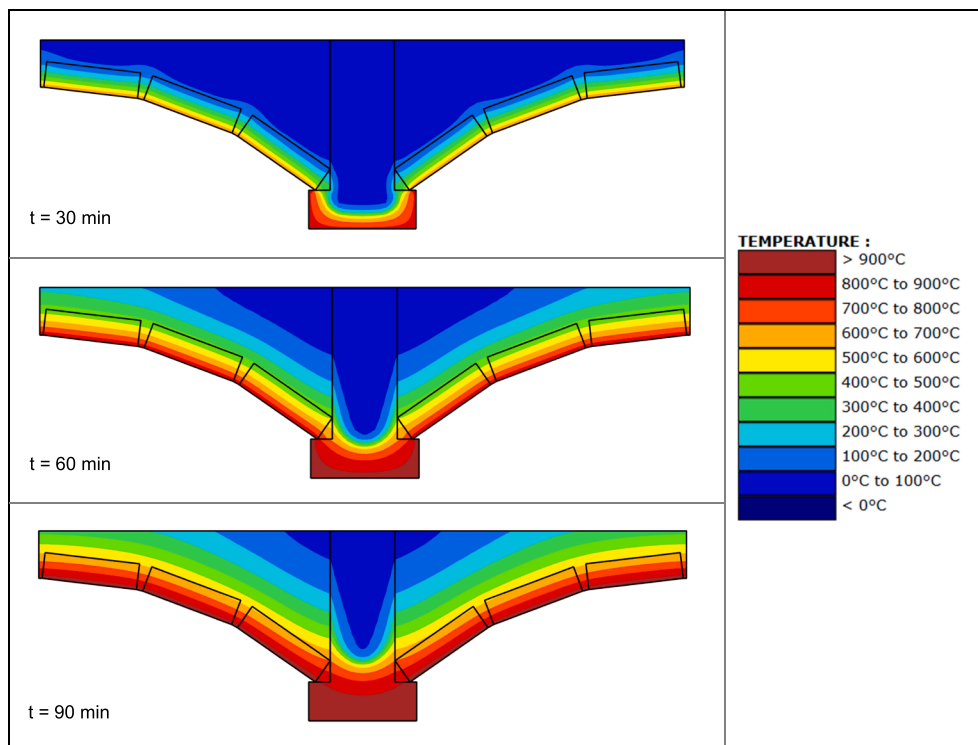


Fig. 16. Temperature fields on the flooring system cross-section for the standard ISO 834 fire exposure at 30, 60 and 90 min. Timber areas with temperatures equal or higher than 300-degrees are theoretically charred.

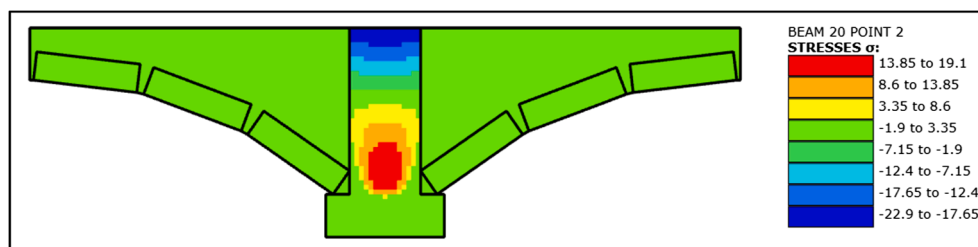


Fig. 17. Normal stresses (in MPa) at mid-span of the flooring system, for the standard ISO 834 fire exposure at 60 min.

maximum temperature values reached within the compartment in comparison to compartments 1 and 2, which makes them more unfavourable. The degree of compliance of the flooring system with the standards is shown in Fig. 19 through safety factors (*SF*) depending on the time of exposure to the different fire models considered. If failure of the brick vaults does not happen, fire resistance time is fulfilled for all fire models considered, since the flooring system is capable of resisting

the fire exposure for more than 60 min. If failure due to the loss of support of the brick vaults is assumed to happen according to the criteria expressed in Fig. 15, then fire resistance of the system decreases significantly: 43 min for the ISO 834, 27 min for P-3a, 34 min for P-3b, 45 min for O-3a and 37 min for O-3b. These values do not meet CTE's [36] fire resistance requirement. However, and as mentioned in Section 4.2.1., collapse of the brick vaults of the specimen occurred 140 min

Table 5

Fire resistance of the timber joist for different fire exposures. If the fire resistance time is not reported, it means that the timber joist did not collapse after 150 min.

Fire exposure	Advanced (SAFIR)	Reduced cross-section 135-degree isotherm	Reduced cross-section 200-degree isotherm	Reduced properties
ISO 834	108.46 min	108.58 min	123.47 min	133.02 min
P-3b	105 min	103.25 min	145.80 min	-
O-3b	121 min	111.23 min	-	-

after the experimental test began, well after timber strips had charred (see Fig. 7c and Fig. 13) and when the charring front was quite advanced. Therefore, these results highlight the need to conduct thermo-mechanical tests on this typology of historical flooring systems to properly establish the criteria and conditions under which this failure mode occurs.

It is worth noting that, the deepest positions of the 135-degree and the 300-degree isotherms are achieved after a certain time of reaching the maximum temperature of the corresponding natural fire and, therefore, time after entering the cooling phase. This fact leads to a reduction of the cross-section load bearing capacity even during the cooling phase. This is clearly observed in Fig. 19, where the safety factors continue to decrease after the natural fires reach their maximum temperatures. Therefore, the direct application of the simplified mechanical methods included in EN 1995-1-2 [40] without any modification for reproducing the behaviour of timber under natural fires also needs to be checked vis-à-vis the inclusion of the effects of the propagation of the thermal wave inside the timber elements during the cooling phase.

In addition, a comparison between the charring depths obtained according to EN 1995-1-2 [40] and those obtained from the 300-degree isotherm in SAFIR [49,50] for the ISO 834 fire exposure has been carried out. Given that the expressions proposed by EN 1995-1-2 [40] apply to standard ISO 834 fire exposure, the charring depths values obtained are compared with the results of SAFIR's [49,50] thermal model associated with the standard ISO 834 fire exposure. EN 1995-1-2 [40] calculations are done assuming a design notional charring rate under standard ISO 834 fire exposure (β_n) of 0.8 mm/min. This value of β_n is associated with solid softwood with a characteristic density greater than 290 kg/m³. The

design notional charring rate (β_n) has been assumed instead of the one-dimensional design charring rate (β_0) as the timber joist is exposed to fire on three sides instead of one.

The result of the comparison is shown in Fig. 20. As can be deduced from the chart, from about 45 min onwards, the value of β_n is no longer valid, probably because the section goes from being exposed to fire on three sides to only one and the joist boundary thermal conditions change. Considering β_0 instead of β_n after the first 45 min would lead to even higher section modulus values, as the value of the β_0 is always lower than β_n . Therefore, the reason why the charring rate increases is that, even though the timber cross-section is, from that moment, exposed to fire only on one side, both the bricks and the infill keep heating the lateral sides of the timber joists at high temperatures (see Fig. 16). In addition, since the cross-section width is smaller, the effect of

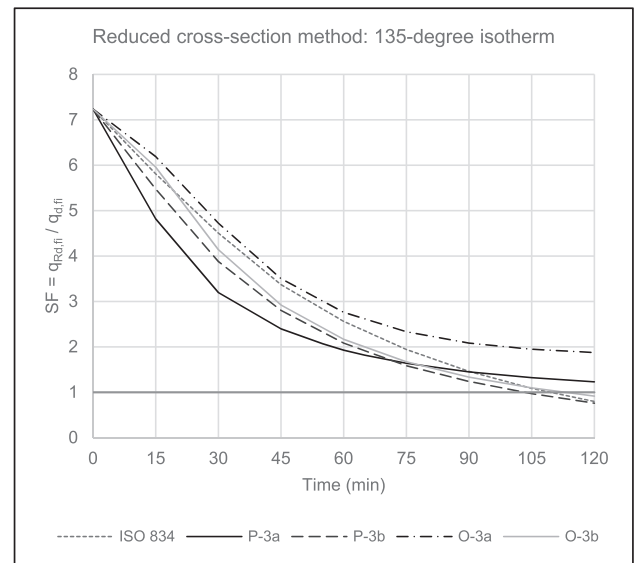


Fig. 19. Safety factors of the flooring system, depending on the time of fire exposure, for the most unfavourable fire models. Results are conditional on failure due to the loss of support of the brick vaults not occurring.

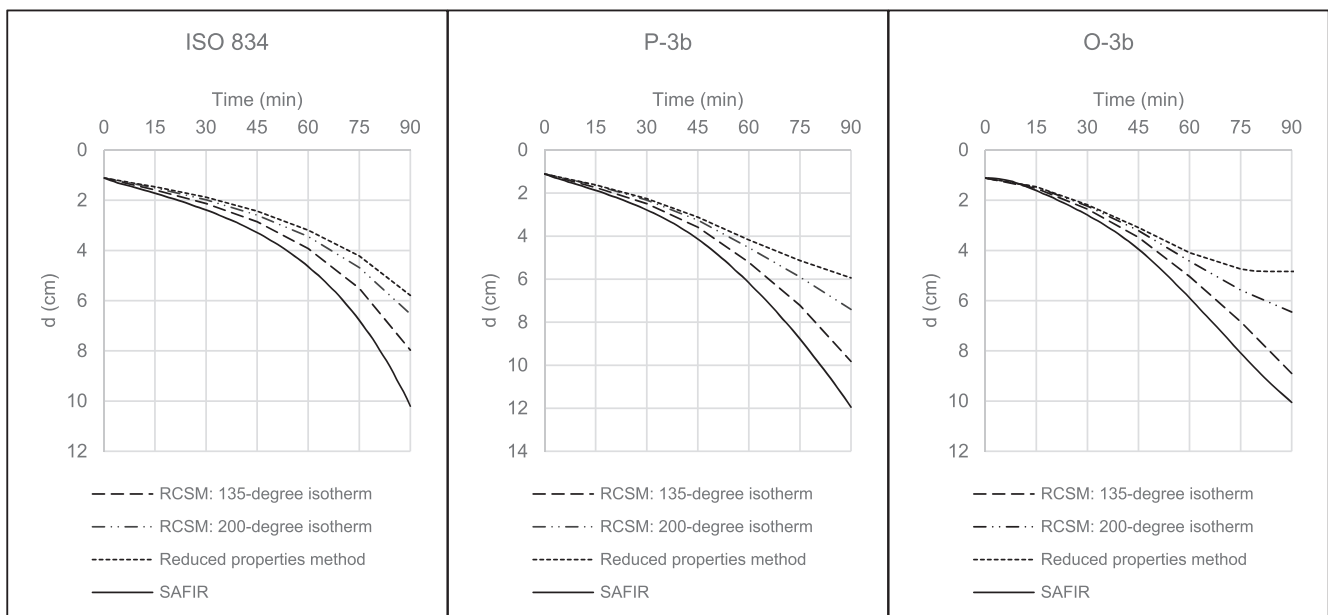


Fig. 18. Mid-span timber joist deflection for the standard ISO 834, P-3b and O-3b fire exposures obtained with the mechanical methods used. Results are conditional on failure due to the loss of support of the brick vaults not occurring.

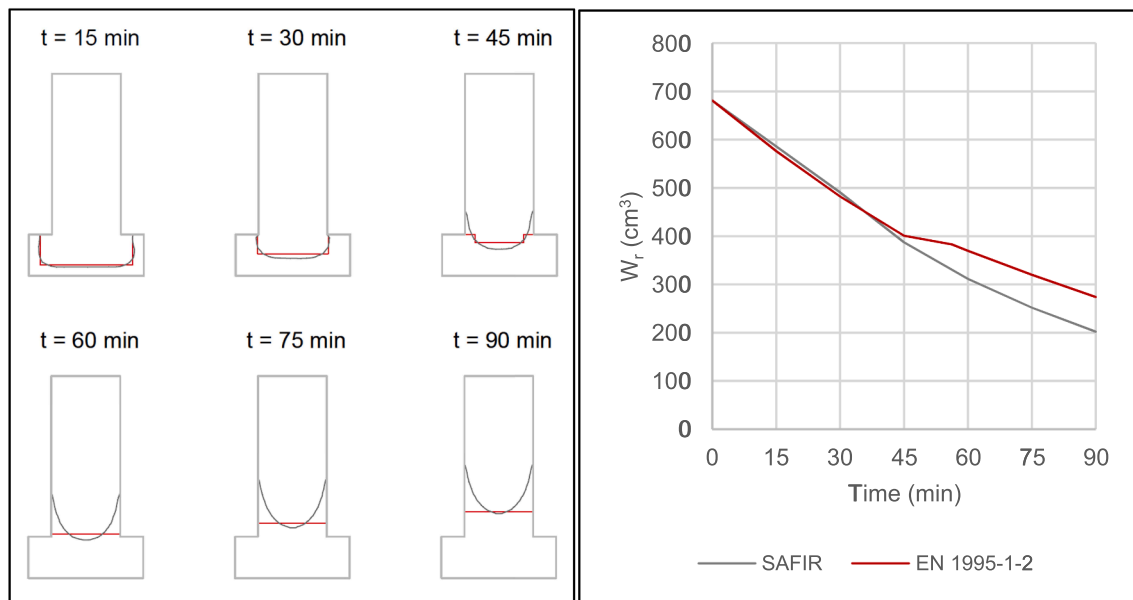


Fig. 20. Variation of timber joists' charring depth with time according to both SAFIR [49,50] (grey lines) and simplified formulation of EN 1995-1-2 [40] (red lines) for the standard ISO 834 fire exposure. W_r is the section modulus of the residual cross-section. (For interpretation of the references to colour in this figure legend, the reader is referred to the web version of this article.)

corner roundings, which consists of increased charring near corners, is more pronounced.

In short, it can be concluded that the charring depths proposed by EN 1995-1-2 [40] underestimate the values predicted by SAFIR [49,50] for this specific type of flooring system. Thus, due to the peculiarities of the cross-section of a timber jack arch flooring system, an alternative method of analysis to verify the fire resistance of these flooring systems is required, as the analytical model for charring of EN 1995-2 [40] is not valid.

6. Parametric study

In this section, a parametric study of the fire resistance time of the flooring system is carried out considering, for different types of fire exposure and several values of timber characteristic static bending strength and span-length. The values considered for the span-length of the flooring system are 3, 4 and 5 m, which are within the usual range.

Concerning the timber strength, its value is, in most cases, unknown, since historical buildings were built many years ago and data is not available. Furthermore, performing mechanical tests to determine it is difficult since the tests could seriously weaken the flooring system.

Alternatively, the values proposed by UNI 11119 [64] standard can be assumed for the strength and stiffness properties of the timber joists. This standard is commonly used for the evaluation of existing timber structures and allows, through visual grading as well as an on-site diagnosis based on the use of non-destructive testing, to assign the mechanical properties of the timber structural element.

For pine wood species, UNI 11119 [64] suggests considering a value of static bending strength equal to 8, 10 or 12 MPa depending on the category assigned to the timber element after visual inspection. According to UNI 11119 [64], the values of elastic modulus associated to these bending strengths are 11000, 12000 and 13000 MPa, respectively.

Additionally, values of characteristic static bending strength of 14, 16, 18 and 20 MPa have also been considered, which correspond to the lower strength classes included in EN 338 [65]. The mean values of modulus of elasticity ($E_{m,0,mean}$) associated to these bending strengths are 7000, 8000, 9000, y 9500 MPa, respectively. It should be noted that the design strength in fire ($f_{d,fi}$) as well as the design modulus of elasticity in fire ($E_{d,fi}$) depend on the coefficient k_{fi} , which, according to EN

1995-1-2 [40], takes a value equal to 1.25 for solid timber.

Once the parameter values are defined, an advanced mechanical analysis in SAFIR [49,50] and a simplified mechanical analysis using the proposed adaptation of the "Reduced cross-section method" are performed.

First of all, Fig. 21 shows the evolution of the effective cross-section's section modulus (W_e) throughout the time of fire exposure for the most unfavourable fire models. It should be recalled that the effective cross-section is associated with the "Reduced cross-section method". As can be observed, leaving aside the additional failure criterion due the loss of support of the brick vaults, P-3a, P-3b and O-3b are the most unfavourable fire models to verify CTE's [36] requirement of fire resistance duration at 60 min since they predict the lowest section modulus values at that specific instant of time.

Next, the maximum fire resistance duration (FR) is obtained for all possible combinations of span length, characteristic bending strength and fire models considered. Fig. 22 summarises the results of the parametric study carried out. As can be observed, the fire resistance

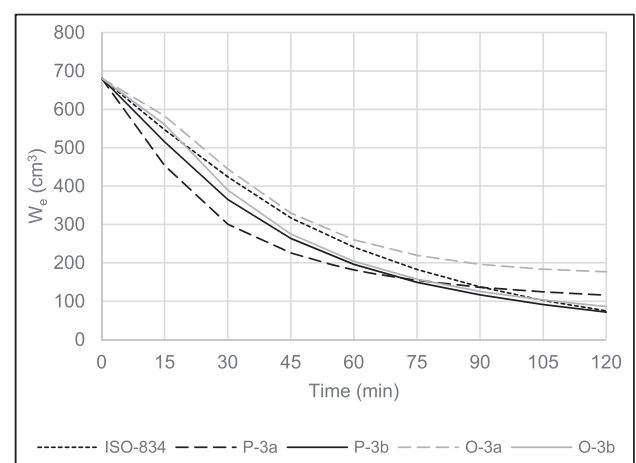


Fig. 21. Section modulus of the effective cross-section (W_e), depending on the time of fire exposure, for the most unfavourable fire models. W_e is obtained using the 135-degree isotherm.

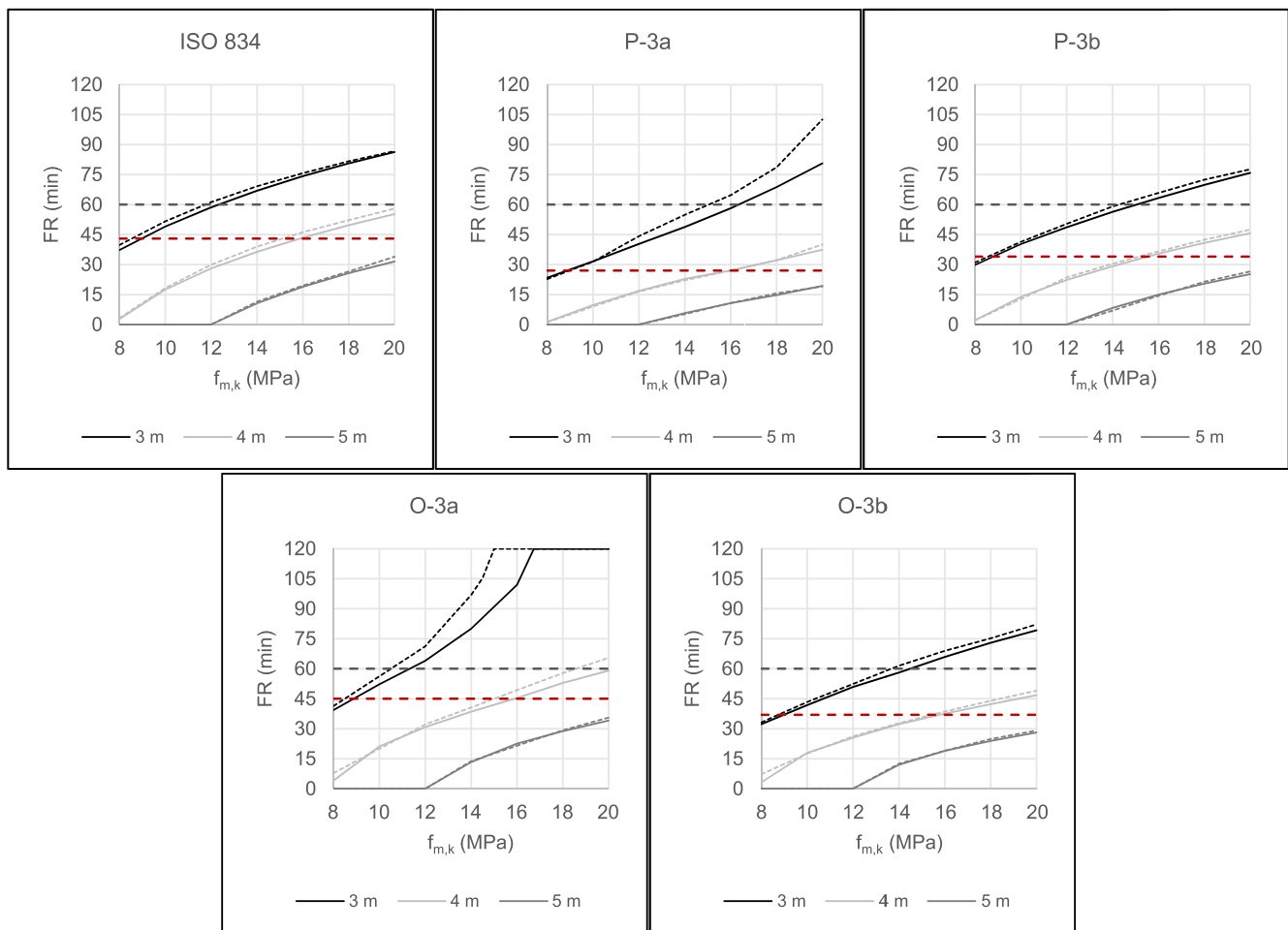


Fig. 22. Fire resistance (FR) of the flooring system as a function of the span-length and timber characteristic bending strength, according to the proposed adaptation of the “Reduced cross-section method” (solid line) and SAFIR’s [49,50] mechanical models (dashed line). Horizontal red dashed lines are estimates of failure times associated to the loss of support of the brick vaults, whilst horizontal grey lines represent CTE [36] requirement of a fire resistance duration of 60 min. (For interpretation of the references to colour in this figure legend, the reader is referred to the web version of this article.)

durations obtained in SAFIR [49,50] are very similar to those obtained in the simplified mechanical method. Once again, it can therefore be concluded that the proposed adaptation of the “Reduced cross-section method” with the 135-degree and 300-degree isotherms is supported by the results given by the advanced mechanical models. Fig. 22 also includes horizontal red dashed lines to mark failure times corresponding to the loss of support of the brick vaults. This lack of support failure time can be smaller than the timber joist mechanical failure. Therefore, conclusions drawn for the results shown in Fig. 22 regarding the parametric study carried out are conditional on failure due to the loss of support of the brick vaults not occurring. It is important to highlight that, given that the standard ISO 834 fire exposure lacks a decay phase, the effective cross-section gradually reduces as the position of the 135-degree isotherm progresses. Conversely, both parametric and OZone curves reach a maximum temperature during the heating phase which is followed by the decay phase. Therefore, as discussed in Section 5, when assuming a natural fire model, the potential deepest position of the 135-degree isotherm in the timber joist cross-section is reached after having reached the maximum temperature of the fire curve, since the wood continues to burn inside. Note also that the deepest position of the 135-degree isotherm, which is associated with the smallest effective cross-section, will be different for each fire exposure and will occur for different times of fire exposure. Bearing this in mind, the slope discontinuity observed in the FR- $f_{m,k}$ curve of Fig. 22 corresponding to case O-3a with a span-length of 3 m is due to the fact that, from a certain value

of timber characteristic bending strength, the joist is able to withstand the fire action considering the smallest effective cross-section and, consequently, the joist is capable of resisting the fire exposure throughout its entire duration (not only 120 min as represented in Fig. 22).

7. Conclusions and future work

This paper has analysed the fire resistance of a historical timber jack arch flooring system subjected to different fire models contemplated by EN 1991-1-2 [38]. For this purpose, both thermal and mechanical analyses have been carried out in SAFIR [49,50]. In addition, a fire test was performed to calibrate the thermal model. Additionally, an adaptation of the “Reduced cross-section method” of EN 1995-1-2 [40] has been proposed to allow its use in timber cross-sections with singular geometries as the one studied. Lastly, a parametric study has been conducted to evaluate the influence of the fire model, the span length and the timber static bending strength on the fire resistance of the historical flooring system. From the analyses performed, the following conclusions can be drawn:

- The calibration of the thermal model in SAFIR [49,50] from the experimental test results has led to the conclusion that the temperature-dependent density and conductivity proposed by EN 1995-1-2 [40] adequately predict the experimental curves. However,

the Wang et al. [53] specific heat curve has been assumed instead of that proposed by EN 1995-1-2 [40] to take into account the actual moisture content of wood, since it has been observed that the thermal model is quite sensitive to this variable.

- The calibrated thermal model developed allows the simulation of the evolution of temperatures on the historical flooring system cross-section and charring in the timber joists under the experimental test fire exposure. Given that the thermal model essentially assumes the thermal properties of EN 1995-1-2 [40] for wood, which are associated with the standard ISO 834 fire exposure, it is expected to reproduce the thermal behaviour of the historical flooring system under the standard ISO 834 fire exposure with accuracy. Results and conclusions regarding the natural fires considered should be taken as indicative, although significant information can be derived from them.
- The standard ISO 834 fire exposure was expected to be, a priori, the most restrictive fire model, as it lacks a decay phase. Nevertheless, it gives unsafe results compared to some cases of both parametric and OZone curves, which predict more unfavourable charring depths. Conversely, the standard ISO 834 could be a too conservative and unrealistic fire model when compared to other cases of these natural fire models. Consequently, it is highly important to assume fire models that depend on the actual physical conditions of the compartments, since they are more realistic and, in some cases, the effects of these fire models on wood charring are more severe than those produced by the standard ISO 834 fire exposure.
- For both parametric and OZone curves, it can be inferred that, under the same ventilation hypothesis, the larger the compartment size, the higher the temperatures reached within it and the longer the duration of the heating phase. Regarding the ventilation conditions, it does not seem obvious whether having fire curves with higher maximum temperatures, but shorter durations of the heating phase is more unfavourable than having lower maximum temperatures but longer durations of the heating phase. Therefore, all possible fire scenarios must be carefully analysed to choose the most severe fire curve when evaluating the fire resistance of a structure. However, in view of the results, under the same ventilation conditions, parametric curves seem slightly more restrictive than OZone curves.
- The simplified methods proposed by EN 1995-1-2 [40] are not able to predict the fire resistance of timber jack arch flooring systems. Consequently, an adaptation of the “Reduced cross-section method” of EN 1995-1-2 [40] has been proposed. The adaptation is based on the use of the 135-degree and the 300-degree isotherms to obtain the positions of the zero-strength layer and the charring depths. The strategy is validated using advanced mechanical models developed in SAFIR [49,50] for a wide range of span lengths, timber bending strengths and fire exposures. In addition, the proposed adaptation allows the consideration of non-standard fire models and, through additional studies, could be applied to other timber structural systems. Therefore, it opens new paths for the application of performance-based approaches in the assessment of the fire resistance of timber structures.
- Fire resistance assessment of timber structural elements heated with natural fires should consider both the heating and the decay phases of the fire due to the propagation of the thermal wave inside the timber element after the fire peak temperature has been reached.
- The values of bending strength proposed by UNI 11119 [64] and assumed for the parametric study, are much lower than those obtained experimentally. That is why, in many cases of the parametric study, the flooring system does not meet the regulatory requirements. In addition, the parametric study makes quite clear that a span length of 5 m is excessive for such low values of timber bending strength.
- Despite the fact that the UNI 11119 [64] provides very conservative values for the timber bending strength, the advantage of using this standard is that the weakening of the flooring system is avoided as

neither destructive nor load tests are required to obtain the mechanical properties of the timber. However, it is likely that, by assuming such low strength values, many existing historical buildings do not meet the regulatory requirements and, therefore, reinforcement or fire protection measures would be required.

- Results of the mechanical analyses carried out, including those of the parametric study, are conditional on the failure due to the loss of support of the brick vaults not occurring. The thermal test performed highlights the need to conduct thermo-mechanical tests on this typology of historical flooring systems to properly establish the criteria and conditions under which this failure mode would occur.

To sum up, this paper proposes a strategy to analyse the fire resistance of historical timber jack arch flooring systems. Thus, the aim of the analysis is twofold: firstly, to promote the preservation of these historical flooring systems and, consequently, the architectural heritage of a country; and secondly, to reduce the environmental impact caused by construction.

Future research should study different wood species since there is a significant variability between their charring rates. In general, the charring rate decreases with increasing wood density as well as increasing moisture content [63,66]. Additional tests with different fire loads and with mechanical loading are also advisable to experimentally validate the mechanical models used, to study the criteria and conditions under which the failure due to the loss of support of the brick vaults occurs and to study the use of passive fire protection such as intumescent paints on the timber joists. Further research should also include the use of probabilistic approaches to consider, among others, the dispersion of timber thermal and mechanical properties and uncertainties related to the charring depth and the zero-strength layer. In addition, future work should also contemplate the development of a simplified calculation method, also including the thermal component, that allows the fire resistance of this type of historical flooring systems to be obtained, and avoids resorting to the development of advanced numerical thermal models. Finally, and to promote the use of performance-based approaches in the fire design of timber structures, it is very important to develop expressions for wood thermal properties for natural fires including the cooling phase that can be implemented in the software packages widely used in structural fire design.

Declaration of Competing Interest

The authors declare that they have no known competing financial interests or personal relationships that could have appeared to influence the work reported in this paper.

Acknowledgements

The authors wish to express their gratitude to the Spanish Ministry of Economy, Industry and Competitiveness for the funding provided through Project BIA 2014-59036-R. This research is also supported by the Spanish Ministry of Science, Innovation and Universities through the PhD grant FPU18/00726 awarded to the first author. Finally, the authors want to thank Prof. Dr. Juan Patricio Hidalgo for his help and MSC Enrique Serra for his assistance in the experimental test.

References

- [1] United Nations - Department of Economic and Social Affairs - Population Division. World Population Prospects 2019: Highlights. New York: UN; 2019. DOI: 10.18356/13bf5476-en.
- [2] United Nations - Department of Economic and Social Affairs - Population Division. World Urbanization Prospects 2018: Highlights. New York: UN; 2019. DOI: 10.18356/6255ead2-en.
- [3] Alba-Rodríguez MD, Martínez-Rocamora A, González-Vallejo P, Ferreira-Sánchez A, Marrero M. Building rehabilitation versus demolition and new construction: Economic and environmental assessment. *Environ Impact Assess Rev* 2017. <https://doi.org/10.1016/j.eiar.2017.06.002>.

- [4] Larsen KE, Marstein N. Conservation of historic timber structures. *Int Symp Wood Sci Technol* 2000.
- [5] Brennan M, Deora A, Heegaard A, Lee A, Lubell J, Wilkins C. Comparing the Costs of New Construction and Acquisition-Rehab In Affordable Multifamily Rental Housing: Applying a New Methodology for Estimating Lifecycle Costs; 2013.
- [6] Gernay T, Elhami Khorasani N, Garlock M. Fire fragility curves for steel buildings in a community context: a methodology. *Eng Struct* 2016;259–76. <https://doi.org/10.1016/j.engstruct.2016.01.043>.
- [7] Gernay T, Khorasani NE, Garlock M. Fire fragility functions for steel frame buildings: sensitivity analysis and reliability framework. *Fire Technol* 2018. <https://doi.org/10.1007/s10694-018-0764-5>.
- [8] Rackauskaite E, Kotsovinos P, Jeffers A, Rein G. Structural analysis of multi-storey steel frames exposed to travelling fires and traditional design fires. *Eng Struct* 2017. <https://doi.org/10.1016/j.engstruct.2017.06.055>.
- [9] Alos-Moya J, Paya-Zaforteza I, Hospitaler A, Loma-Ossorio E. Valencia bridge fire tests: validation of simplified and advanced numerical approaches to model bridge fire scenarios. *Adv Eng Softw* 2019. <https://doi.org/10.1016/j.advengsoft.2018.11.003>.
- [10] Albero V, Saura H, Hospitaler A, MontalvÀ JM, Romero ML. Optimal design of prestressed concrete hollow core slabs taking into account its fire resistance. *Adv Eng Softw* 2018. <https://doi.org/10.1016/j.advengsoft.2018.05.001>.
- [11] Ji J, Tong Q, (Leon) Wang L, Lin CC, Zhang C, Gao Z, et al. Application of the EnKF method for real-time forecasting of smoke movement during tunnel fires. *Adv Eng Softw* 2018. DOI: 10.1016/j.advengsoft.2017.10.007.
- [12] Bergmeister K, Brunello P, Pachera M, Pesavento F, Schrefler BA. Simulation of fire and structural response in the Brenner Base Tunnel by means of a combined approach: a case study. *Eng Struct* 2020. <https://doi.org/10.1016/j.engstruct.2020.110319>.
- [13] Bernardi P, Michelini E, Sirico A, Rainieri S, Corradi C. Simulation methodology for the assessment of the structural safety of concrete tunnel linings based on CFD fire – FE thermo-mechanical analysis: a case study. *Eng Struct* 2020. <https://doi.org/10.1016/j.engstruct.2020.111193>.
- [14] Pallares-Muñoz MR, Paya-Zaforteza I, Hospitaler A. A new methodology using beam elements for the analysis of steel frames subjected to non-uniform temperatures due to fires. *Structures* 2021;31:462–83. <https://doi.org/10.1016/j.istruc.2021.02.008>.
- [15] Rafi MM, Aziz T, Lodi SH. A suggested model for mass fire spread. *Sustain Resilient Infrastruct* 2020. <https://doi.org/10.1080/23789689.2018.1519308>.
- [16] Ferreira TM, Baquedano P, Graus S, Nochebuena E, SocarrÀs T. Evaluaci3n de riesgo de incendio urbano en el centro hist3rico de la ciudad de GuimarÀes. *Inf La Construcci3n* 2018;70:262. <https://doi.org/10.3989/ic.58962>.
- [17] Torero JL. Fire safety of historical buildings: principles and methodological approach. *Int J Archit Herit* 2019. <https://doi.org/10.1080/15583058.2019.1612484>.
- [18] Pratiç3 Y, Ochsendorf J, Holzer S, Flatt RJ. Post-fire restoration of historic buildings and implications for Notre-Dame de Paris. *Nat Mater* 2020;19:817–20. <https://doi.org/10.1038/s41563-020-0748-y>.
- [19] Deldicque D, Rouzaud J-N. Temperatures reached by the roof structure of Notre-Dame de Paris in the fire of April 15th 2019 determined by Raman paleothermometry. *Comptes Rendus Géosciences* 2020. DOI: 10.5802/crgeos.9.
- [20] Chorlton B, Gales J. Fire performance of cultural heritage and contemporary timbers. *Eng Struct* 2019. <https://doi.org/10.1016/j.engstruct.2019.109739>.
- [21] Chorlton B, Gales J. Fire performance of heritage and contemporary timber encapsulation materials. *J Build Eng* 2020. <https://doi.org/10.1016/j.jobe.2020.101181>.
- [22] Lineham SA, Thomson D, Bartlett AI, Bisby LA, Hadden RM. Structural response of fire-exposed cross-laminated timber beams under sustained loads. *Fire Saf J* 2016. <https://doi.org/10.1016/j.firesaf.2016.08.002>.
- [23] Schmid J, Klippel M, Just A, Frangi A, Tiso M. Simulation of the Fire Resistance of Cross-laminated Timber (CLT). *Fire Technol* 2018. <https://doi.org/10.1007/s10694-018-0728-9>.
- [24] Wiesner F, Bisby LA, Bartlett AI, Hidalgo JP, Santamaria S, Deeny S, et al. Structural capacity in fire of laminated timber elements in compartments with exposed timber surfaces. *Eng Struct* 2019;179:284–95. <https://doi.org/10.1016/j.engstruct.2018.10.084>.
- [25] Klippel M, Frangi A. Fire safety of glued-laminated timber beams in bending. *J Struct Eng (United States)* 2017. [https://doi.org/10.1061/\(ASCE\)ST.1943-541X.0001781](https://doi.org/10.1061/(ASCE)ST.1943-541X.0001781).
- [26] Richter F, Kotsovinos P, Rackauskaite E, Rein G. Thermal response of timber slabs exposed to travelling fires and traditional design fires. *Fire Technol* 2021;57:393–414. <https://doi.org/10.1007/s10694-020-01000-1>.
- [27] Bartlett AI, Hadden RM, Bisby LA. A review of factors affecting the burning behaviour of wood for application to tall timber construction. *Fire Technol* 2019. <https://doi.org/10.1007/s10694-018-0787-y>.
- [28] Schmid J, Santomaso A, Brandon D, Wickstr3m U, Frangi A. Timber under real fire conditions – the influence of oxygen content and gas velocity on the charring behavior. *J Struct Fire Eng* 2018. <https://doi.org/10.1108/JSFE-01-2017-0013>.
- [29] Astier H. Notre-Dame: Massive fire ravages Paris cathedral. *BBC News* 2019. <https://www.bbc.com/news/world-europe-47941794> (accessed September 17, 2020).
- [30] Brazil's national museum hit by huge fire. *BBC News* 2018. <https://www.bbc.com/news/world-latin-america-45392668> (accessed September 17, 2020).
- [31] Glasgow fire: Art school's Mackintosh building extensively damaged. *BBC News* 2018. <https://www.bbc.com/news/uk-scotland-glasgow-west-44504659> (accessed September 17, 2020).
- [32] Neves IC, Valente JC, Branco FA. Study of the Chiado fire in Lisbon. *Proc Inst Civ Eng Struct Build* 1995. <https://doi.org/10.1680/istbu.1995.27869>.
- [33] UN. United Nations Transforming Our World: the 2030 Agenda for Sustainable Development. A/RES/70/1. 2015.
- [34] Diodato M, Macchioni N, Brunetti M, Pizzo B, Nocetti M, Burato P, et al. Understanding Spanish timber jack arch floors: examples of assessment and conservation issues. *Int. J. Archit. Herit*. 2015. <https://doi.org/10.1080/15583058.2015.1041193>.
- [35] Diodato M. Estudio hist3rico de la madera arquitect3nica en la ciudad de Valencia. Análisis previos para la conservaci3n y puesta en valor: identificaci3n de maderas, análisis constructivo, diagn3stico, clasificaci3n y dendrocronología. *Universitat Politècnica de València* 2015. <https://doi.org/10.4995/Thesis/10251/58606>.
- [36] Ministerio de Vivienda. C3digo Tècnico de la Edificaci3n (CTE). *Real Decreto 314/2006* 17 Marzo 2006. DOI: CTE-DB-SE.
- [37] HM Government. The Building Regulations 2010 - Approved Document B - Fire Safety: Volume 1 - Dwellings. England: 2019.
- [38] European Committee for Standardization (CEN). Eurocode 1: Actions on structures - Part 1-2: General actions - Actions on structures exposed to fire. Brussels, Belgium: 2002.
- [39] ISO 834-1. Fire-resistance tests - Elements of building construction - Part 1: General requirements; 1999.
- [40] European Committee for Standardization (CEN). Eurocode 5: Design of timber structures - Part 1-2: General - Structural fire design. Brussels, Belgium; 2004.
- [41] European Committee for Standardization (CEN). Eurocode 6: Design of masonry structures - Part 1-2: General rules - Structural fire design. Brussels, Belgium; 2005.
- [42] Poon LS, He Y. Experimental Observations and Modelling of Window Glass Breakage in Building Fires; AOFST Symp. 3; 1988.
- [43] Cadornin JF, Franssen JM. A tool to design steel elements submitted to compartment fires - OZone V2. Part 1: Pre- and post-flashover compartment fire model. *Fire Saf J* 2003. [https://doi.org/10.1016/S0379-7112\(03\)00014-6](https://doi.org/10.1016/S0379-7112(03)00014-6).
- [44] Cadornin JF, Pintea D, Dotreppe JC, Franssen JM. A tool to design steel elements submitted to compartment fires - OZone V2. Part 2: methodology and application. *Fire Saf J* 2003. [https://doi.org/10.1016/S0379-7112\(03\)00015-8](https://doi.org/10.1016/S0379-7112(03)00015-8).
- [45] Franssen JM. Improvement of the parametric fire of Eurocode 1 based on experimental test results. *Fire Saf Sci* 2000. <https://doi.org/10.3801/IAFSS.FSS.6-927>.
- [46] Albero V, Serra E, Espin3s A, Romero ML, Hospitaler A. Innovative solutions for enhancing the fire resistance of slim-floor beams: thermal experiments. *J Constr Steel Res* 2020;165. <https://doi.org/10.1016/j.jcsr.2019.105897>.
- [47] O'Neill JW, Buchanan AH, Abu AK, Carradine DM. *The Fire Performance of Timber Floors in Multi-Storey Buildings*. Doctoral Thesis. University of Canterbury; 2013.
- [48] Su J, Lafrance P-S, Hoehler M, Bundy M. Fire Safety Challenges of Tall Wood Buildings - Phase 2: Tasks 2 & 3 – Development and Implementation of CLT Compartment Fire Tests. *Natl Fire Prot Assoc* 2018.
- [49] Franssen JM. SAFIR: A thermal/structural program for modeling structures under fire. *Eng J* 2005;42:143–50.
- [50] Franssen J-M, Gernay T. Modeling structures in fire with SAFIR: theoretical background and capabilities. *J Struct Fire Eng* 2017;JSFE-07-2016-0010. DOI: 10.1108/JSFE-07-2016-0010.
- [51] European Committee for Standardization (CEN). EN 408:2010+A1:2012 - Timber structures - Structural timber and glued laminated timber - Determination of some physical and mechanical properties. Brussels, Belgium: 2012.
- [52] European Committee for Standardization (CEN). EN 13183-1:2002 - Moisture content of a piece of sawn timber - Part 1: Determination by oven dry method. Brussels, Belgium: 2001.
- [53] Wang Y, Burgess I, Wald F, Gillie M. Performance-based fire engineering of structures. 2012. DOI: 10.1201/b12076.
- [54] Rinaudo P, Paya-Zaforteza I, Calder3n PA. Improving tunnel resilience against fires: a new methodology based on temperature monitoring. *Tunn Undergr Sp Technol* 2016. <https://doi.org/10.1016/j.tust.2015.11.021>.
- [55] Kuehnen RT, Youssef MA. Equivalent standard fire duration to evaluate internal temperatures in natural fire exposed RC beams. *Fire Saf J* 2019. <https://doi.org/10.1016/j.firesaf.2019.102831>.
- [56] K3nig J, Walleij L. One-dimensional charring of timber exposed to standard and parametric fires in initially unprotected and postprotection situations; 1999.
- [57] Friguin KL. Material properties and external factors influencing the charring rate of solid wood and glue-laminated timber. *Fire Mater* 2011. <https://doi.org/10.1002/fam.1055>.
- [58] European Committee for Standardization (CEN). Eurocode 1: Actions on structures - Part 1-1: General actions - Densities, self-weight, imposed loads for buildings. Brussels, Belgium; 2002.
- [59] European Committee for Standardization (CEN). Eurocode - Basis of structural design. Brussels, Belgium; 2002.
- [60] Franssen J-M, Gernay T. User's manual for SAFIR 2019 - Mechanical. A computer program for analysis of structures subjected to fire. Liège, Belgium: University of Liege. Department ArGenCO. Service Structural Engineering; 2019.
- [61] Huc S, Pecenko R, Hozjan T. Predicting the thickness of zero-strength layer in timber beam exposed to parametric fires. *Eng Struct* 2021. <https://doi.org/10.1016/j.engstruct.2020.111608>.
- [62] Schmid J, Just A, Klippel M, Fragiaco M. The reduced cross-section method for evaluation of the fire resistance of timber members: discussion and determination of the zero-strength layer. *Fire Technol* 2015. <https://doi.org/10.1007/s10694-014-0421-6>.
- [63] Hurlay MJ, Gottuk D, Hall JR, Harada K, Kuligowski E, Puchovsky M, et al. SFPE handbook of fire protection engineering, fifth edition. 2016. DOI: 10.1007/978-1-4939-2565-0.

- [64] Ente Nazionale Italiano di Unificazione - Commissione "Beni culturali – NORMAL." Norma italiana UNI 11119. Beni culturali. Manufatti lignei. Strutture portanti degli edifici – Ispezione in situ per la diagnosi degli elementi in opera. Milano (Italy): 2004.
- [65] European Committee for Standardization (CEN). EN 338:2016 - Structural timber - Strength classes. Brussels, Belgium: 2016.
- [66] Cachim PB, Franssen JM. Comparison between the charring rate model and the conductive model of Eurocode 5. Fire Mater 2009. <https://doi.org/10.1002/fam.985>.